

N68-21915

FACILITY FORM 602

(ACCESSION NUMBER) _____ (THRU) _____

62 (PAGES) _____ (CODE) _____

CF-72371 (NASA CR OR TMX OR AD NUMBER) _____ (CATEGORY) 33

Experimental Investigations of Liquid Propellant Combustion Processes Using Streak Photography

by

Richard M. Williams, Jr.

GPO PRICE \$ _____

CFSTI PRICE(S) \$ _____

Hard copy (HC) 3.00

Microfiche (MF) 1.5

ff 653 July 65

prepared for

NATIONAL AERONAUTICS AND SPACE ADMINISTRATION
Contract NASr 217

February 1968

Department of Aerospace
and Mechanical Sciences
PRINCETON UNIVERSITY



NOTICE

This report was prepared as an account of Government sponsored work. Neither the United States, nor the National Aeronautics and Space Administration (NASA), nor any person acting on behalf of NASA:

- A.) Makes any warranty or representation, expressed or implied, with respect to the accuracy, completeness, or usefulness of the information contained in this report, or that the use of any information, apparatus, method, or process disclosed in this report may not infringe privately owned rights; or
- B.) Assumes any liabilities with respect to the use of, or for damages resulting from the use of any information, apparatus, method or process disclosed in this report.

As used above, "person acting on behalf of NASA" includes any employee or contractor of NASA, or employee of such contractor, to the extent that such employee or contractor of NASA, or employee of such contractor prepares, disseminates, or provides access to, any information pursuant to his employment or contract with NASA, or his employment with such contractor.

Requests for copies of this report should be referred to

National Aeronautics and Space Administration
Office of Scientific and Technical Information
Attention: AFSS-A
Washington, D.C. 20546

TECHNICAL REPORT

EXPERIMENTAL INVESTIGATIONS
OF LIQUID PROPELLANT COMBUSTION PROCESSES
USING STREAK PHOTOGRAPHY

by

Richard M. Williams, Jr.

approved by

Luigi Crocco and David T. Harrje

prepared for

NATIONAL AERONAUTICS AND SPACE ADMINISTRATION

February 1968

CONTRACT NASr-217

Technical Management
NASA Lewis Research Center
Cleveland, Ohio
Chemistry and Energy Conversion Division
Marcus F. Heidmann

Guggenheim Laboratories for the Aerospace Propulsion Sciences
Department of Aerospace and Mechanical Sciences
Princeton University
Princeton, New Jersey

TABLE OF CONTENTS

TITLE PAGE	Page i
TABLE OF CONTENTS	ii
FOREWORD AND ACKNOWLEDGEMENTS	iii
SUMMARY	iv
SYMBOL TABLE	v
INTRODUCTION	vii
I. COLD FLOW STUDIES	1
II. ROCKET MOTOR STUDIES	17
APPENDIX A: Techniques of Streak Photography	31
APPENDIX B: Application of Streak Photography to Rocket Combustion Studies	35
REFERENCES	46
LIST OF FIGURES	49
FIGURES	

FOREWORD AND ACKNOWLEDGMENTS

This technical report represents both an examination of a previously reported phenomenon and the initiation of a new experimental test program for the study of combustion processes within a rocket motor. Both phases of this research program involved the use of streak-camera photography with the results serving as an illustration of the versatility and usefulness of a streak camera. The cold flow program evolved from preliminary work concerning droplet wave phenomenon, as described in Reference 1. The rocket motor research program is concerned with a new technique of determining the steady-state chamber properties and with the application of streak photography to a research rocket motor. Described herein is the preliminary study of the experimental program associated with this research. It should be noted that this work and the results reported are preliminary, with the principle investigations planned for the future.

Support for this research was provided by NASA under Contract NASr-217.

The author wishes to thank Mr. D.T. Harrje for his valuable assistance during the entire effort of this research, and also Mr. Victor Warshaw and Mr. Kenneth Gadsby along with other members of the Guggenheim Laboratories Staff for their efforts in the design, fabrication and operation of much of the experimental apparatus. Also deserving of much thanks is Mrs. Evelyn Olsen for her patience and effort in the typing of this report. The analytical work involved with the pulse techniques of chamber property analysis were and are being continued under the direction of Mr. Frediano Bracco.

SUMMARY

Measurements of droplet breakup wave frequency were taken under a variety of experimental conditions. These included measurements with 90° impinging jet injectors of several orifice diameters, pressure drops up to 150 psi and involved several fluids. The data resulting from streak photographs were empirically correlated to give a relationship between frequency, chamber pressure, and other pertinent parameters. Application of the empirical relationship to actual rocket motor data with intermediate frequency range pressure oscillations resulted in a linear data fit, thereby supplying some support to the association of impinging jet breakup and intermediate frequency combustion pressure oscillations.

In addition to this cold flow study, the initiation of an experimental program to study combustion processes is described. This research, which will be continued, was concerned with combustion processes within the rocket motor and was principally associated with experimental inputs to an analytical study of steady combustion. Unsteady combustion was studied with both streak photography and pressure transducers. The resulting velocity and pressure data at various axial locations together with other results tended to confirm that the research motor was quite similar to the one-dimensional model.

SYMBOL TABLE

		UNITS
a	speed of sound $= \sqrt{\frac{\partial p}{\partial \rho}} = \sqrt{\gamma RT}$	(ft/sec)
a*	critical speed of sound $= \sqrt{v_{r1} v_{r2}}$	(ft/sec)
A	area	(in ²)
	- empirical constant	
c*	characteristic exhaust velocity	(ft/sec)
D	diameter	(in)
E	internal energy relative to 298°K	(ergs)
f	frequency of droplet wave phenomenon	(cps)
g	gravitational acceleration of Earth	(ft/sec ²)
H	enthalpy	(ergs)
L	length	(in)
	- dimensional length unit	
M	object to image film magnification factor	
	- Mach number	
	- dimensional mass unit	
P	stagnation pressure	(psi)
p	static pressure	(psi)
Q	heat added to warm liquids to vaporization temperature	(ergs)
Q _v	heat of vaporization	(ergs)
q	dynamic pressure	(psi)
R	resistance factor, related to friction coefficient	(psi)
T	stagnation temperature	(°K)
	- dimensional time unit	
t	static temperature	(°K)
U	shock velocity	(ft/sec)
v	velocity	(ft/sec)
w	fluid flow rate	(#/sec)
x	axial coordinate	
M	molecular weight	
R	universal gas constant	
α	streak angle	
η _c *	combustion efficiency based on c*	

UNITS

γ	- ratio of specific heats	
k	- gas coefficient of thermal conductivity	(cal/cm sec ^o K)
μ	- viscosity	(#sec/ft ²)
ρ	- density	(#/ft ³)
σ	- surface tension	(#/ft)
$\frac{\partial}{\partial x}$	- partial derivative with respect to the x dimension	
$\frac{\partial}{\partial t}$	- partial derivative with respect to time	
$\frac{\partial}{\partial p}$	- partial derivative with respect to pressure	
$\frac{\partial}{\partial \rho}$	- partial derivative with respect to density	

SUBSCRIPTS

c	- chamber
exp	- experimental
F	- fuel
f	- film
g	- gas
I	- injector
L, l	- liquid
r	- relative to shock
x	- axial direction
t	- throat
th	- theoretical
0	- at injector
1	- immediate vicinity in front of shock
2	- immediate vicinity behind shock
ϕ	- oxidizer

SUPERSCRIPTS

a - g, c_1 - c_4 - empirical exponents

INTRODUCTION

In the study of liquid propellant rockets a thorough knowledge of the combustion processes is of primary importance. Here at Princeton studies of this nature are of interest to the research effort in liquid rocket combustion instability. Associated with any experimental research efforts in this area are various experimental techniques and tools. One technique which has been found to be of great use in the past in the study of shock waves and flame propagation is streak camera photography, a tool primarily used for velocity measurements. This report describes its application to both cold and hot-flow studies. The cold-flow study is concerned with impinging jet instability and its possible association with combustion instability. The hot-flow study is concerned with more fundamental aspects of combustion and is primarily involved with steady-state chamber properties. This study involves the use of a new technique which incorporates the use of a shock pulse within the rocket combustion chamber.

The cold-flow study was conducted in a chamber geometrically similar to actual rocket hardware. An imposed flow of gas was also supplied and was intended to simulate the generation of combustion gases, while the chamber pressure was designed to duplicate the densities actually present in rocket combustors.

The primary objective of the cold-flow study was further understanding of the mechanisms involved with the generation of droplet population waves from an impinging jet injector. Streak photography was the primary tool used in measuring the frequency of these droplet waves, the frequency and hence wavelength being of ultimate concern with regard to the possibility of this phenomenon becoming a trigger for combustion instability.¹¹

The hot-flow study involves the use of an experimental rocket motor which operates on LOX/Ethyl Alcohol with chamber pressures up to 900 psi and a thrust of 800 lbs.

The principal object of this investigation is a further understanding and a more accurate knowledge of the various properties within

the combustion chamber during steady-state operation. Again streak photography is used, this time in conjunction with a diagnostic technique incorporating a shock pulse. Ultimately it is hoped that through a better understanding of the steady-state combustion process more can be learned about unsteady combustion, specifically the mechanism of energy addition associated with combustion instability.

I. COLD FLOW STUDIES

Purpose

The study of liquid spray characteristics has been and continues to be of prime importance in the quest for knowledge and understanding of liquid propellant combustion processes. Early investigations were previously concerned with application to internal combustion engines.^{7,8,9} Recent studies of spray characteristics have been directed toward application in liquid propellant rocket engines.^{1,5,6}

As reported in Ref. 1, variations in droplet population, as seen in spark photomicrographs, were tentatively associated with periodic variations in the spray breakup pattern (Fig. 1). However, for such variations to be deducible from a number count based on spark photographs with the dimensions used in this study, the frequency would necessarily be in the 100-200 Hz range. It should be noted at this point that these oscillations were observed with no pressure oscillations within the chamber and with no detectable oscillations in the feed system. In previous work^{5,6} the frequency associated with this effect, designated the "Christmas Tree" effect or "Pagoda" effect, was on the order of 1000-2000 cps. The only difference in the operating conditions associated with these other investigations is that the high frequency results were observed with ambient pressure while the low frequencies found in the research at Princeton were found under conditions of significant chamber pressure (100 psig)*. Further investigation of this phenomenon was felt to be warranted on the basis of its possible association with both intermediate frequency, "buzz", and high frequency, "screaming", combustion instability.¹¹ In addition to the observation of impinging jet instability, a similar phenomenon has also been reported for sheets formed by liquid jets on curved surfaces.¹⁰

The primary purpose of this research was to carry out an experimental investigation of the phenomenon with the hope that the experimental results would lead to an analytical treatment of the problem and hence a physical explanation of the occurrence.

* This cold flow chamber pressure corresponds to a chamber density equal to that found in a LOX/Ethanol rocket operating at 1500 psi.

Experimental Apparatus

This section, dealing with the experimental apparatus used to conduct the investigation, will be divided between two topics:

1) the testing facilities and 2) the recording facilities. The first topic includes the cold flow chamber, which is designed to simulate certain conditions in an actual rocket combustion chamber, and the feed systems associated with this chamber. The discussion of the recording apparatus will include the photographic technique and equipment, associated lighting system, and devices for various physical measurements (i.e. flow rates, chamber pressure and liquid injection pressure). A photograph and schematic of the experimental apparatus can be seen in Figs. 2 and 3.

The simulated combustion chamber is a six-inch diameter horizontal cylindrical chamber 20" long, and is capable of operation up to a chamber pressure of 150 psig.* The test section consists of three pairs of quartz windows mounted on each side of the chamber and occupying the first 4" of the chamber from the injector. Recent modifications have made it possible to replace the three separate windows with one large lucite window. (Fig. 4) Downstream of this position are located two more windows for possible studies at positions far from the injector, however, these windows were not employed in the present study. Further downstream is a plexiglas section whose length can be varied and hence permit variations in the longitudinal resonant frequency of the chamber. For the tests to be described here the chamber was maintained at a length which corresponded to a resonant frequency of 340 cps.

The two injectors used for this investigation were mounted at one end of the test chamber. These were 90° like-on-like impinging jet injectors ("doublets") with orifice diameters of .040 and .059 inches. The design of these injectors, as seen in Fig. 5, is similar to those used in other phases of instability research at Princeton and indeed in actual rocket motors. The elliptical spray fans (Fig. 1) resulting from these injectors were aligned so as to present the major axis normal to the optical path, hence the major axis was in a vertical position. At

* This limitation is imposed by the available nitrogen supply for the flow rates used in these tests.

the location where streak photographs were taken (approximately 2" from the injector) the spray fan had a width of about 1/2".

The test chamber was pressurized with nitrogen gas flow which was introduced into the chamber through circumferential slots around the windows. This design was used to protect the windows from the spray so that liquid on the windows would not degrade the photographic results. This technique of gas injection was entirely adequate for tests using the separate windows, however, for those tests conducted with the single lucite window, liquid collection in the window was quite severe except at low chamber pressures, a fact which indicates the presence of strong recirculation currents. The use of side injection of the nitrogen may, however, provide simulation of the generation of combustion products from adjacent injectors.

Due to significant cooling of the nitrogen when expanded from its 1600 psi supply into the chamber a hot water heat exchanger was necessary. This kept the chamber at nearly ambient temperature, thus preventing external fogging of the window and problems of ice formation within the chamber.

The exhaust system in the chamber consisted of six 1/4" holes spaced circumferentially at the end of the plexiglas section. A plate behind this could be rotated to vary the true exit area from the equivalent of two holes to the full six holes. This plate kept the flow as uniform as possible. Behind this was a siren used to produce pressure oscillations within the chamber. However, for all but a few tests this was clamped in the open position. The primary purpose of the variable exit area plate was to permit tests to be made under steady and unsteady conditions with the same nitrogen flow rates, which was accomplished by increasing the exit area for unsteady tests. In the tests of this investigation an equivalent exit area of 3 holes was used (this corresponds to a nitrogen flow rate of about .35 #/sec at $p_c = 100$ psig).

The test liquids used were water, a mixture of 50% water and 50% methyl alcohol, 100% methyl alcohol and water with a surface tension reducing agent (surfactant). These were stored in a nitrogen pressurized tank of capacity 25 gallons and pressure limit 500 psi. After injection the test fluid was exhausted through a hole at the bottom of the siren

end of the chamber. Injection pressure drops were varied from 50 to 150 psi with corresponding injection velocities of 60 and 105 ft/sec.

The principal experimental data recording technique used in this investigation was that of streak photography. This technique allowed the variations in droplet number density to be seen as a function of time. Data on size-velocity relationships could also be obtained from this technique, although this data is not directly applicable to the phenomenon being investigated. The optical arrangement used in this study was direct photography as contrasted to Shadowgraph or Schlieren techniques. A schematic of the setup can be seen in Fig. 3. The camera itself was simply a box with two film guide spools and one film drive sprocket, as seen in Fig. 6. This allowed an 80" continuous loop of 35 mm film to be used for data recording. Located in close proximity to the film, as it passed over the sprocket drive, was a horizontal slit of variable width (the usual width was $1/32"$). The film represented the point of focus of droplets in the center of the chamber, with a moveable, f-3.5, 200 mm lens supplying the focusing mechanism. The streak camera was placed parallel to the test chamber due to room size restrictions resulting from the magnification used (5.2). The magnification used did not result from any direct requirements of this investigation, but simply because the system had been previously used in the study of droplet-size distributions.¹ Directly behind the telephoto lens was a shutter which was synchronized with the film velocity so that most of the film loop was exposed. The light source used was a high pressure Mercury arc lamp. This provided a constant, high intensity source of radiation for adequate exposure of the film. Since direct photography was employed, no collimation of the light beam was required, however, due to considerations of film exposure the beam had to be kept narrow, especially when one considers the long focal length of the camera and the film speed (up to 130 ft/sec).

An accurate determination of the film velocity was obtained through the use of a time light signal generator which exposed one edge of the film with a 500 cps oscillation. This signal was triggered by the shutter and hence would give a true picture of the film velocity at the time the data was recorded.

Various alternatives of film and developer were considered or

tried due to the critical lighting conditions under which these streak pictures were taken.¹² Kodak Recording 2475 (Royal-X Pan Recording), Kodak Tri-X and Ansco Super Hypan film were tried with various developing times and temperatures in Microdal-X, DK-60A, D-8, D-19, DK-50, D-76 and Baumann two-bath Diafiore developer. Due to the large percentage of ultraviolet radiation in the mercury arc, orthochromatic film with ultraviolet sensitivity and Kodak Spectrum Analyses plate film #1 were considered but eliminated for reasons of expense. Also considered were techniques of increasing the sensitivity of the silver halide emulsion, but were eliminated due to excessive time requirements. Finally Kodak 2475 (formerly Royal-X Pan Recording) film was selected with development in DK-50 for 8 minutes. This was chosen primarily because of its high speed (ASA 1600). Mercury and chromium intensifiers were also tried on the film negatives, but with little success since the limits of the film had already been approached.

The secondary recording apparatus consisted of various pressure gages for liquid injector and chamber steady pressures. In addition to these, unsteady measurements were made to confirm that the droplet wave phenomenon was not caused by feed system oscillations. These measurements were carried out through the use of a Kistler 601 pressure transducer and an electromagnetic flow meter.*

For still pictures of the first three inches of the spray a standard film holder back with separate shutter was used in conjunction with the same telephoto lens. In this case, however, the magnification was on the order of one, so that more of the spray could be photographed. For these pictures a mechanical shutter would not be sufficiently fast to "stop" the droplets, thus a spark source of duration approximately 1 μ sec was used which provided sufficient light for exposure. A piece of frosted glass between the spray and the light source was used to diffuse the relatively narrow light beam from the spark and hence illuminate the spray uniformly over the first three inches extending from the injector face. These pictures, as seen in Fig. 7, were intended to provide a better overall picture of the spray breakup. Polaroid type 52 film was used for these tests, primarily because of its 10 second development time so that the

* Designed at JPL and reported in Reference 47.

tedious and time consuming process of film development was eliminated.

Experimental Procedure

Because of the number of parameters that influence the jet breakup process the initial experiments were directed toward determining the governing factors. A choice was made as to what were the important parameters while the results of the preliminary testing were used to check the assumption of which of these was important and to determine in what manner they affected the wave-like spray breakup pattern. The independent variable was taken to be the frequency of the spray breakup, where the frequency was defined as the average over many cycles of the phenomenon. The primary variable chosen was the chamber pressure since it was the apparent change in wave frequency with pressure which initiated the desire for further study. Additional variables were: 1) injector size, 2) injection velocity (pressure drop), 3) liquid density, 4) liquid viscosity and 5) liquid surface tension. An additional important parameter may be the gas viscosity but no easily employed means were available for changing this property.* It is interesting to note that Giffen and Neale⁸ indicated no appreciable effect of gas viscosity on the spray atomization (i.e., on the droplet size distribution). From these parameters a series of tests were planned to study the effect of each (where possible) on the frequency of breakup. The injector sizes available were .040 and .059 inches. The injection velocity was varied by changing the pressure drop across the injector, where nominal values were 50, 100 and 150 psi. Different liquids were used to change the fluid properties. The following table lists these liquids and their effects on the various physical properties with respect to the values of water.

<u>Properties -</u>	Density	Viscosity	Surface Tension
<u>liquids</u>	(#/ft ³)	(#f-sec/ft ²)	(#f/ft)
water	1 (62.4)	1 (2.09x10 ⁻⁵)	1 (5x10 ⁻³)
50% water-50% methyl alcohol	.93	1.86	.48
methyl alcohol	.80	.6	.31
water surfactant	1	1	.41

* N₂, air and He differ in viscosity by only about 10% within the temperature range normally encountered in the test apparatus.

The normal test sequence called for a series of four runs with the test liquid and orifice size being the same for each. The tests were then run at four different chamber pressures (normal range was 20 to 100 psig) while the injector pressure drop was maintained constant by increasing the injection pressure along with the chamber pressure. The shutter speed was set so as to nearly completely expose the film, both to the injector spray and the time light. After each run the film loop had to be removed from the spools and replaced with an unexposed loop. This was accomplished readily in an undarkened room by the use of a changing bag attached to the side of the camera. This side of the camera was also capable of being slid back to reveal the inside of the camera to facilitate the necessity of aligning the camera and of loading and removing film cans before and after each test sequence.

After completion of one or more test sequences the resulting exposed film had to be processed. This procedure was the most time consuming part of the data recording. Thirty minutes were required to develop two loops of film. Thus each test sequence required one hour of continuous attendance before any useable results could begin to be obtained from the tests. This time factor led to the consideration of other techniques of data recording.

The immediately obvious technique is to eliminate the need for film, and hence the associated developing, by employing a photoelectric device of some sort. The initial thought was that as each wave of droplets passed in front of the device, its electrical output would change, thus giving a direct plot of droplet density vs. time. After initial tests using a simple Cadmium Sulfide photoconductive cell, it was seen that this technique would not be as simple as it seemed. The first fault found in this technique was that the photocell was "seeing" every individual droplet, rather than waves of droplets. This led to a very noisy signal from which little useful results could be obtained. The next approach was to place a piece of frosted glass between the spray and photocell so that the individual droplets would not be viewed. However, under those conditions the photocell could not distinguish between a group of small droplets and one large droplet. Next it was decided that advantage

might be taken of the photocells' ability to see each droplet. The ultimate aim being that of a system which would give the complete spray history at any point in the spray. This theoretically meant that not only could the grouping phenomena be studied but also that information on size and velocity distribution could be obtained. However, again the technique was beset with problems. The principal one being that the recording system could not respond quickly enough as a droplet passed by. Included in the recording system were the photocell and a tape recorder, with the latter being the most restrictive since it only had a frequency response of 10 KHz. In the light of these problems and the lack of time available for their solution, it was decided to return to the more tedious, but perfected, recording technique of streak photography. However, the author still feels that the technique has merit and with more sophisticated equipment, and time, could yield the desired data, thus resulting in a great saving of time and effort in certain studies of liquid sprays.

The experimental procedure for recording data of a large portion of the spray involved the use of the previously described camera arrangement. The same parameters remained important and were studied. However, this time a spark photograph of the spray was taken. This yielded a still picture of the spray structure which clearly showed the droplet wave and grouping phenomenon, an example of which can be seen in Figure 7. From this picture and the droplet velocities as measured from the previously obtained streak photographs, the frequency of droplet grouping could be determined. This technique would yield fairly precise results if the velocities were accurately known. However, since the streak photographs taken earlier were intended for direct measurement of the grouping frequency, the streaks were kept in a nearly vertical position. This meant that for velocity measurements small errors in the measurement of the streak angle would result in large errors in the streak velocity. Thus this technique can only be considered qualitatively useful in describing the significant, initial portion of the spray.

Data Reduction

Subsequent to a relevant experiment and the employment of proper photographic techniques, the main task of data reduction must be faced.

In this case the streak photographs obtained had to be reduced in such a way that the droplet population density phenomenon could be analyzed. This meant that some form of a number density vs. time curve was sought. The initial method chosen to achieve this was to divide the streak film into small segments representing a certain time period and to then count the number of droplets (or streaks) within each interval. This procedure was carried out by hand and was quite time consuming and tedious, although simple. However, its time consumption represented a major drawback (along with film development time) to the experimental effort. This then gave the motivation for seeking other forms of data procurement (photocells) as discussed earlier and other forms of data reduction (to be discussed later). Through a visual observation of the film one could detect the various regions of droplet densities, however, it was felt that this simple procedure was not accurate enough since the droplet density variations were far from sinusoidal.

The first step involved in "hand count" reduction of the streak film was the choice of a suitable time interval over which to count streaks. It was decided from the two limits already known of the phenomenon (i.e., frequency of variation ≈ 2000 cps @ $p_c = 0$ psig^{5,6} and frequency ≈ 100 cps @ $p_c = 100$ psig¹) that the time interval would be taken as one-fourth the expected period at each chamber pressure, with the assumption of frequency = 0 cps @ $p_c = \infty$, so that an inverse power law decay was assumed for frequency as a function of chamber pressure. Thus for tests under conditions of different chamber pressures the time interval was chosen differently. One-fourth of the period was chosen so that enough droplet counts were contained in the interval and so that the interval would not be comparable to the period. After these counts were taken from each streak film the results were plotted, number vs. time. The resulting curve showed cyclic variation. The next decision was to use the average frequency, over all the cycles recorded on film, to characterize the spray breakup under the conditions of that particular test run. Thus the final result of the photographic data reduction is a table containing the frequency of droplet number density variations for the various test conditions. A plot of frequency vs. chamber pressure for the various conditions can be seen in Figure 8. The other independent variable measured was the ratio of the number of droplets in the wave

maximum to that in the wave minimum. This was done to check for the existence and extent of any possible resonance effects. However, there was found to be very little effect, with the ratio remaining at an approximate value of between 2 and 3 for all conditions, including resonant conditions, though it should be noted that the streak photographic technique is probably not sensitive enough to note a small effect. Resonance effects were checked by operating at that chamber pressure which was found to yield a droplet breakup frequency equal to the chamber resonant frequency. Again it should be noted that in only these tests were there pressure oscillations, and that the phenomenon appeared unaffected by the oscillation, as opposed to other results¹³ which showed a coupling. However, this other work involved pressure oscillations of 30% whereas the oscillations induced for this data were no more than 10%. Also the impinging jet droplet variations of this other work were attributed to interactions between the pressure and liquid jets before impingement. The design of the injectors used in these tests (Fig. 5) precludes such an interaction since the jets impinge at the injector face. Perhaps the photoelectric technique discussed earlier could obtain better results regarding resonance effects.

From the data thus obtained it was decided to formulate an empirical relation, through the use of dimensional analysis, to fit the observed points. This approach assumed the spray breakup frequency to be a function of chamber pressure, injector orifice diameter, injection velocity, and the liquid properties of density, viscosity and surface tension. Also included was the gas viscosity even though this property could not be significantly varied. Thus we have:

$$f = f(p_c, D_I, v_I, \rho_l, \mu_l, \sigma_l, \mu_g) \quad (\text{I-1})$$

or

$$f = A D_I^a \rho_l^b v_I^c \sigma_l^d \mu_l^e p_c^f \mu_g^g \quad (\text{I-2})$$

considering dimensions

$$\frac{1}{T} = L^a \frac{M^b}{L^{3b}} \frac{L^c}{T^c} \frac{M^d}{T^{2d}} \frac{M^e}{L^e T^e} \frac{M^f}{L^f T^{2f}} \frac{M^g}{L^g T^g}$$

$$\begin{aligned}
 \text{balancing dimensions} \quad M:0 &= b+d+e+f+g \\
 L:0 &= a-3b+c-e-f-g \\
 T:-1 &= -c-2d-e-2f-g
 \end{aligned} \tag{I-3}$$

$$\begin{aligned}
 \text{or} \quad a &= -(1+d+e+g) \\
 b &= -(d+e+f+g) \\
 c &= 1-2d-e-2f-g
 \end{aligned} \tag{I-4}$$

thus

$$f = A \frac{v_x}{D_T} \left(\frac{\sigma_x}{D_T \rho_x v_x^2} \right)^{c_1} \left(\frac{\mu_x}{D_T \rho_x v_x} \right)^{c_2} \left(\frac{\rho_x v_x^2}{P_c} \right)^{c_3} \left(\frac{\mu_g}{\mu_x} \right)^{c_4} \tag{I-5}$$

or

$$\frac{f D_T}{v_x} = A \left(\frac{\sigma_x}{D_T \rho_x v_x^2} \right)^{c_1} \left(\frac{\mu_x}{D_T \rho_x v_x} \right)^{c_2} \left(\frac{\rho_x v_x^2}{P_c} \right)^{c_3} \left(\frac{\mu_g}{\mu_x} \right)^{c_4} \tag{I-6}$$

Now using the test data one gets the exponents, $c_1 - c_4$ to be -.25, 3.25, .8, and 2.9 respectively. In Fig. 9 can be seen the final empirical plot of all data. The constant A is determined from the slope of the best linear fit to be $A = 2 \times 10^{16}$. Thus the final empirical relationship is:

$$\frac{f D_T}{v_x} = 2 \times 10^{16} \left(\frac{\sigma_x}{D_T \rho_x v_x^2} \right)^{-.25} \left(\frac{\mu_x}{D_T \rho_x v_x} \right)^{3.25} \left(\frac{\rho_x v_x^2}{P_c} \right)^{.8} \left(\frac{\mu_g}{\mu_x} \right)^{2.9} \tag{I-7}$$

Also seen in Fig. 9 is a curve resulting from data obtained from transverse rocket tests^{2,3} and plotted with the same empirical relationship. Again we get a straight line but now the constant is greatly different. The explanation of this is that the gas viscosity is much larger in the rocket motor tests than in the cold flow study and since this property has not been previously analyzed the large change shows up as a major variation in the empirical constant. However, even with the constants not being equal the straight line curve fit of the rocket motor tests lends some credence to the postulate that the droplet wave phenomenon can be a cause

of combustion instability in the intermediate frequency range. Also, if this correspondence is correct we see that perhaps a factor in $(\frac{\mu_g}{D_T \rho_L \nu_L})^{C_5}$ would be appropriate for the empirical relationship.

Definite phase relationships can be seen in the pressure traces of runs in which intermediate frequency combustion instability occurred (Fig. 10). These are different from those found in the presence of acoustic oscillations and hence can not be acoustically explained. It might be postulated that phasing effects between adjacent spray fans, as related to the spray breakup phenomenon, are associated with these phase relationships, but this would only be speculation since such effects were not studied in the cold flow testing.

The next step in this study was to investigate more suitable means of film data reduction than hand counting. It was felt that if a record could be made of each droplet (or streak) and its position (or time) relative to some reference that complicating effects of various droplet sizes and velocities could be reduced. This was accomplished by slowly moving the film at constant speed past a backlight and having the operator put a marker on a moving strip recorder. The operator was necessary to insure that all size droplets were equally counted. The same data was simultaneously processed by an analog to digital converter with the result being a card punched for each droplet with its time from a certain reference. Thus any test would result in a stack of cards, representing consecutive droplets in the spray and having punched on them the time of passage of each droplet through the optical axis of the photographic system. With this data it was then hoped that the computer could somehow resolve the droplet number density variations into an average frequency.

Before proceeding with the computer techniques it should be stated that the strip chart trace of the raw streak film data could be visually checked for droplet grouping. They appeared more clearly than on the film itself since no account was taken of droplet size in the strip chart recording whereas when one viewed the streak film the natural tendency was to see the larger droplets. When visually observing the strip chart recordings the droplet groups could be detected and an average frequency computed which fell near the values determined by the hand counting technique, but more important than a quantitative check was the qualitative

fact that the grouping frequency did change with varying test conditions, specifically the chamber pressure. Because of the limited number of cycles involved in any of the streak film records only an average frequency of droplet groupings can be determined - the absolute value being subject to errors of the order of $\pm 10\%$. However, the important factor is the well-documented change in this frequency with changing test conditions. The pertinent result for liquid rockets being that under varying conditions the spray breakup instability would occur at different frequencies and that under the proper circumstances this breakup frequency might correspond to the resonant frequency of the rocket and hence could act as a trigger for high frequency combustion instability, a decidedly more destructive type than intermediate frequency or "buzz" instability.¹¹

Let us now return to the computer techniques tried in the reduction of the data. The principal technique used was that of autocorrelations. Here the initial oscillating curve of droplet number vs. time is shifted somewhat and then multiplied by the original curve. After several shifts and suitable normalization a correlation coefficient is obtained, which is a measure of the shifted correspondence with the original curve. Thus a true sine wave would show the correlation coefficient starting at + 1.0, decreasing to - 1.0 and returning to + 1.0 as the curve is shifted one period. However when this technique was applied to the processed streak film data the results were very inconclusive with the primary explanation being that not enough information (cycles) had been recorded on the film. A similar result and explanation were obtained when Fourier analysis of the data was tried. Compounding the lack of information contained on the film was the nonsinusoidal nature of the signal.

Additional techniques were tried but with relatively unsuccessful results. Among these was one which was similar to the hand count technique but which allowed the count interval to be varied for the data of any test. This procedure was impossible when done by hand due to time considerations, however, with the computer it could be done with relative ease. Although this technique substantiated the hand count results within 10%, another lower frequency was also indicated. The first thought was that a degree of feed system coupling was present even though no chamber pressure oscillations were present. However, as was seen previously, high frequency response instrumentation* was not able to detect any oscillations in the

* This instrumentation consisted of an electromagnetic flowmeter and a Kistler 601 pressure transducer mounted as close to the injector as possible, as can be seen in Figs. 2 and 4.

feed system other than random noise.

It was hoped that still pictures would supply a better overall view of the spray breakup pattern so that an explanation of the lack of precise substantiation of the hand count data by the computer could be obtained. And indeed these pictures, as seen in Fig. 7, did supply more information about the jet instability. It is evident that the droplet wave pattern changes markedly with increasing chamber pressure. At high pressures the waves of droplets seem to have degenerated into distinct droplet groups, which would help explain the more or less random groupings seen in streak films. These pictures do, however, again confirm the variation in grouping frequency with chamber pressure, at least for pressures below 60 psig, even though the frequency values as determined from the still pictures are somewhat higher than the hand counted streak film results. Thus the empirical relation derived from the streak technique may not be applicable for chamber pressures above 60 psig.

Results and Conclusions

This section deals with the general results obtained from this study of impinging jet breakup. The final empirical relationship covers a wide range of physical parameters which seem to affect the wave-like breakup phenomenon. The application of intermediate frequency rocket motor data to this relationship indicates a correlation with respect to the frequency of the buzz oscillations. However, this data also reveals a seemingly strong influence of gas viscosity on the phenomenon. Unfortunately this parameter could not be significantly varied with this existing experimental apparatus and hence could not be examined in the cold flow study.

The principal parameter affecting the frequency of droplet breakup is the chamber pressure, even though the dependence is a rather mild one ($p_c^{-.8}$), since in an actual rocket motor the chamber pressure may vary by nearly an order of magnitude. This means that conditions might exist where the droplet breakup frequency corresponds to the combustion chamber resonant frequency. Such a resonant condition could be a possible mechanism of high frequency combustion instability triggering.

Also, as previously discussed, the breakup phenomenon seems to be related to certain intermediate frequency pressure oscillations. This relationship might arise from tangential variations in mass distribution caused by phase differences between adjacent injector elements. Such an occurrence can only be speculated though since phase differences could not be investigated. Also it should be remembered that at chamber pressures above 60 psig (corresponding to about 1100 psia in a LOX/RP-1 combustion chamber) the wave pattern degenerated into groups, rather than waves, or droplets. Thus, if the droplet wave pattern was associated with the intermediate frequency pressure oscillations, tests conducted in the research motors at pressures above 1100 psia should not exhibit any of these pressure oscillations. Unfortunately such tests were not and could not be conducted and hence no definite conclusion can be drawn with regard to the association of the observed droplet breakup and intermediate frequency pressure oscillations.

The most significant physical property, other than gas viscosity, seems to be the liquid density. However, since this parameter does not vary a great deal in applications other than liquid hydrogen combustion, it has little real significance. The other physical properties studied (viscosity and surface tension) showed little effect on the breakup frequency.

This leaves only the injection velocity and injector diameter to be discussed. The frequency seems to depend very little on injection velocity, however the breakup wavelength (i.e., spacing between droplet groups) would depend rather strongly on the injection velocity. In certain respects the breakup wavelength may be of as much importance as the frequency, especially in cases of circumferential phasing between injector jets. The injector orifice diameter has a much stronger effect than velocity upon breakup frequency, which may be a reflection of variations in the droplet sizes.

The general effects of these parameters on spray breakup (primarily drop size distribution) under ambient conditions can be found in References 1, 5, 6, 7, 8 and 9.

In conclusion, it should be stated that this work constituted

an effort to gain a fuller understanding of the wave-like character of the sprays resulting from the impinging jets. The original hope had been that experimental testing would direct the way to an analytical approach to the phenomenon. However, this has not been the case. The experimental program has resulted, in an empirical expression, which does seem to partially correlate with certain intermediate frequency instabilities, but no physical mechanism has been uncovered to explain the phenomenon.

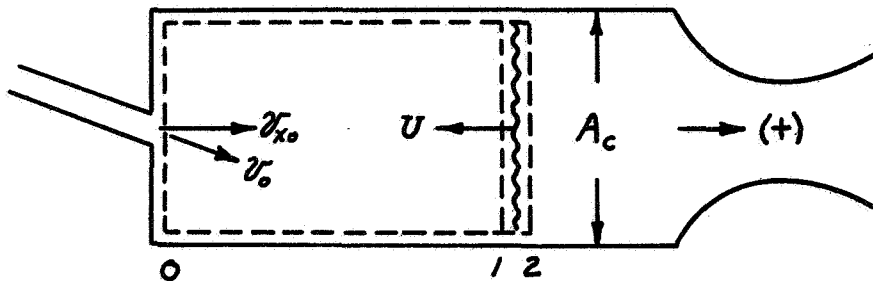
II. ROCKET MOTOR STUDIES

Purpose

Although cold flow studies are quite useful in obtaining a qualitative idea of what would actually occur in a rocket combustion chamber, they are no replacement for the experimental testing of rocket motors. Development of experimental techniques and preliminary tests in the investigation of steady-state combustion processes (including the consideration of gains and losses under unsteady conditions) are discussed in this section.

The ultimate goal of this research is to determine the physical mechanisms governing high frequency combustion instability, specifically the energy feedback mechanisms. However, before such knowledge can be obtained, a thorough understanding of stable combustion processes must be gained. This necessitates an accurate determination of the steady-state chamber properties. The principal technique used for this determination is based upon the use of a shock pulse. A secondary method employed streak photography to measure gas velocities and other combustion parameters subsequently derived from the gas velocity is outlined in Appendix B. The streak photography data, besides supplying qualitative information on such factors as mixture ratio striations, served to verify the shock velocity data obtained from transducers appropriately spaced along the chamber walls.

The shock technique applies the general conservation equations to a steady rocket combustion chamber with a shock moving axially up the chamber.⁴ These equations can be applied between sections 0 and 1 and



again between 1 and 2. This results in a system of six equations which have nine unknowns ($\rho_2, v_2, \rho_1, v_1, p_1, \rho_2, v_2, p_2, U$). Thus, in order for the system to become determinate, three of these unknowns must be measured. Those parameters which at first seem to be the most easily measured are the pressures behind and in front of the shock (p_2 and p_1) and the shock velocity (U). These measurements could be made with several high-frequency response pressure transducers spaced axially along the chamber. Another set of parameters are the gas velocities behind and in front of the shock (v_2 and v_1) and the shock velocity (U). These measurements could be made thru the use of streak photography. Thus we see that two independent means for obtaining a determinate set of equations are available. For a more complete description of the analytical treatment of this technique see Reference 4.

Experimental Apparatus

The primary piece of experimental equipment used for this study was a variable-length, heat-sink cooled, rocket motor, as previously used in other research studies at Princeton.^{2,3,4} A photographic and schematic of the experimental setup can be seen in Figures 11 and 12. This rocket motor normally operates on propellant combinations of either liquid oxygen-ethyl alcohol (LOX/ALC) or liquid oxygen, RP-1 (a fine cut of kerosene). For the initial test to be conducted in conjunction with this study of steady-state combustion the former propellant combination was used. If in the future it is felt that better photographic results are necessary a propellant combination of LOX-Hydrazine will be tried. The basic rocket motor consists of many relatively short length, square sections with a 2.66" square interior. These sections can be combined to obtain variable lengths, with the range extending from 3" to 100", and are held together and sealed by a hydraulic press. In the tests described here the length was maintained at 70 inches, this allowed the combustion to be completed well before the nozzle was reached. However, as will be described later, the length may be changed to 100 inches if it is found that the pulse does not steepen into a normal shock prior to reaching the combustion zone.

The motor is fed with the propellant from nitrogen pressurized tanks with cavitating venturis, flow rate meters, and valves located just upstream of the injector. The spark plug ignition of gaseous oxygen and

gaseous hydrogen is used to initiate combustion of the main propellants. Normal operation involves a nearly constant propellant flow rate of slightly greater than 3#/sec. With this flow rate the chamber pressure was varied (from 150 to 900 psi) by changing the nozzle throat dimension. The injector used for this study was a 4 x 4 array of pairs of like-on-like impinging jets with the spray fans oriented in a diagonal fashion, to control the early mixing of the propellants, as seen in Figure 13.

An important addition to the basic rocket motor was the pulse gun. Previous testing had been done with a simple gun type pulse mechanism normally mounted at the nozzle end of the chamber. That device relied on small quantities (maximum of 45 grains) of fine grain pistol powder which ignited, ruptured a burst disk and hence generated a spherical shock wave at the end of the motor. The shock front then proceeded upstream rapidly approaching the normal shock condition. That type pulse was entirely adequate for inducing instability, however, even with high frequency response pressure instrumentation the amplitude of the pulse was often very difficult to measure accurately since the shock was very steep-fronted (i.e., the pressure rise rate was beyond the capabilities of the pressure instrumentation) and fell off very rapidly after achieving its peak. Combs, in Reference 11, indicated that a similar pressure transducer arrangement could only reach about 60% of the peak amplitude. Since the pressure ratio across the shock is an important and sensitive parameter for the previously defined shock pulse technique, this inaccuracy would prove unacceptable. Thus it was decided to design a pulse which would have the shape of a step-function and hence allow the pressure transducer time to reach the peak amplitude. Another requirement on the pulse was a pressure ratio of 1.2 or greater so that this parameter would be less subject to experimental errors associated with the pressure measurement technique. This meant that a gas flow rate from the pulse gun would have to be instantaneously of the same order as the chamber propellant flow rate and also that this flow rate be maintained for a sufficient time for the pressure instrumentation to respond. Thus instead of a pulse gun, in effect we now have a small, neutral burning, solid propellant rocket on the side of the chamber. An alternate arrangement might be to use a mono-propellant which is forced through a catalyst bed at the desired rate by

a piston. However, the former technique is the only one used in this preliminary study. To insure choked flow into the chamber at a rate of about 3#/sec, the step pulse generator must operate at high pressures (~ 3000 psi). Within the time limitations imposed by the pressure instrumentation it is desirable to keep the pulse duration as short as possible for two reasons: 1) so that the chamber is not maintained at an elevated pressure very long* and 2) so that the total solid propellant charge weight be kept small. The final pulse duration was chosen to be between 5 and 15 milliseconds. The lower pulse time was associated with a rifle powder (Hercules-Reloader #7 and #11) and was used for the higher pulse strength testing. The longer pulse time was associated with larger solid propellant pellets (Hercules 5250.95) as used in the initial pulse checkout and in low pulse strength ($p_2/p_1 \approx 1.2$) testing. Ignition of the pulse charge was accomplished with an electric match imbedded within the charge. If it is decided that the pulse is not steepening into a shock soon enough the motor length can be increased to 100 inches to insure that a proper shock is attained prior to a position 40 inches from the injector, this location corresponds to the position beyond which the window section could not be placed and is sufficiently beyond the region where combustion is active. A picture of the pulse shape, as recorded by Kistler 603A pressure transducers can be seen in Figure 14.**

The instrumentation used in the test runs associated with this experimental study can be conveniently divided into three groups: 1) photographic, 2) fast response pressure transducers and, 3) auxiliary equipment. The auxiliary instrumentation consisted of the commonly used devices for measuring propellant flow rates (Potter meters), various temperatures (thermocouples), and steady-state pressures.

As previously mentioned, the photographic instrumentation for these runs was a streak camera, the same as was used in the cold flow study. However for these tests a different optical setup was used. This was simply the photography of self-luminous sources within the combustion chamber. These sources would either be regions of hot gas or the burning vapor surrounding a droplet. Some thought was given to seeding the combustion chamber,¹⁴ but the idea was rejected since the nonseeded tests yielded vel-

* Based on considerations of window cooling effects and possible leak problems.

** When the appropriate playback compensation circuitry finally arrives for the tape recorder and improved charge amplifiers are used much of the ringing will be eliminated.

ocity results in close agreement with predicted gas velocities. The principal advantage of seeding is that one knows exactly what is being photographed, however, with the propellant combination used for these tests (LOX/Ethyl Alcohol) it was doubtful if optical filtering would permit the seed particles to be seen since available high pressure spectroscopic data for hydrocarbon fuels indicated a continuum emittance by carbon.¹⁵ However, for other propellant combinations seeding might prove very beneficial, at least for qualitative studies. For quantitative studies of the velocity changes in combustion chambers, the seeding particles have to be extremely small (approx. 1μ or less) for them to follow rapid changes in gas velocity.¹⁶ Thus the preliminary decision was to avoid seeding if possible, with the alternative being to switch to a seeded LOX/Hydrazine propellant combination if the streak velocity data obtained was inadequate.

A further modification to the streak photography system used in the cold flow study was the use of a different lens. This change was the result of rocket test cell size restrictions, and restrictions placed upon the accuracy of the velocity measurements from the streak photographs. Since the error involved in obtaining velocity data from streak photographs is a strong function of the streak angle (due to the $\tan \alpha$ dependence) and the fact that the minimum error occurs for angles of 45° it was decided to design the streak photography system so that the streak angles would be on the order of 45° for the velocities of interest. The film velocity is known to within 1%, by means of a timing light, and thus the measurement of the streak angle represents the principal error in the streak velocity determination. In any streak system there are two ways of changing the streak angle for a fixed particle velocity: 1) change the film speed or, 2) change the object to film magnification factor. For the present situation the film speed could not be varied sufficiently to obtain the required change, that is to have a particle (or gas) velocity of 700 ft/sec correspond to a streak with angle 45° . However, the film velocity was increased somewhat (to 125 ft/sec). The magnification factor was chosen to be approximately 1/5. Also it should be noted that the magnification factor of 1/5 allows more detail to be seen than in other researches using the streak photographic technique.^{29,41} If one makes the conservative assumption that the streak angle can be measured to within $\pm 1^\circ$, a curve

of the error in velocity measurement vs. velocity can be plotted (Fig. 15). Also since the 35 mm film used in this streak camera has a useable width of film about 1 inch we know the length of the window slit in the motor necessary to obtain the desired magnification. As can be seen in Fig. 15 the curves for various window lengths (or magnifications) show that different velocity ranges, for a fixed permissible error, are obtained at different magnifications. For a window length of 5 inches ($M = 1/5$) the velocity range is 300-1600 ft/sec for an error of $\pm 5\%$, and 100-3500 ft/sec for an error of $\pm 10\%$. This means that the streak photographs will accurately determine the particles or gas velocities of interest (400-700 ft/sec) and will also give a fairly good value of the shock velocity, even though this is not necessary because it will be accurately measured by the various pressure transducers located axially along the chamber.

The streak camera is actually mounted parallel to the rocket motor which means that a first surface mirror is again used. Also used is a neutral density filter. This was necessary due to the intense combustion light from the motor (approximately 10 times as intense as a mercury arc light). All of this streak system is mounted on a rail parallel to the rocket motor so that it may be moved to different axial locations of the motor. The slit width used in this streak setup was almost .005 inches.

After the window length was determined from consideration of errors involved in streak velocity measurements a new window section had to be designed and built (the previous window was only 1" long). This section had to be about 8" long and mated with the other sections of the rocket motor. With this length, three or four runs are required to obtain a complete velocity profile of the combustion region of the motor. Although these preliminary tests were conducted using self-luminosity, the chamber was machined with 5" slits (1/4") on each side so that high intensity backlighting could be used for future shadow streak pictures if desired. Also incorporated into this section were mounting holes for three fast response pressure transducers. This allows direct comparison of streak pictures with pressure traces as well as giving an accurate value of the shock velocity at the window section. Next, the actual window had to be designed so that it could operate under the conditions associated

with the rocket test firing. Fortunately, run durations were short (approximately 2 seconds) so that this would not be a severe problem. In fact, for runs using the 603A Kistler pressure transducer run durations were only 250 milliseconds for reasons to be described later. Even with short duration tests it was felt that the availability of a nitrogen bleed would be advisable. A photograph of the window section is shown in Fig. 16. Initial tests showed that the lucite windows used were being charred after each two second run, which necessitated replacement. The charring seemed to occur after the onset of instability since it did not seem to affect the window visibility in that portion of the test when the streak photographs were taken. If in the future quartz windows are desired, only a slight modification to the window assembly would be necessary to allow such changes.

The fast response pressure instrumentation previously referred to are Dynisco transducers. These units had to be used in these preliminary test runs while the Kistler Model 603A transducers were being readied to withstand the rocket environment. The Kistler transducers are uncooled and obtain thermal protection from a 1/8 inch* thick ablative coating suitably attached in the copper mounting plug. To limit heat penetration through coatings, the run duration has been limited to 250 ms. Naturally this necessitates the use of an automatic run sequencer rather than depending on human response to properly sequence the necessary events. This sequencer has been checked out and is being used in the tests now employing the Kistler transducers. A new tape recording system (Honeywell 7600) is also being used in the primary testing. This system is now also checked out and will represent a great improvement over the 12-year old Ampex system, which had a frequency response of only 10 KHz. However, the use of Dynisco's and the Ampex have provided adequate data for the initial checkout of the experimental techniques to be used.

Experimental Procedure

Since this study is only the preliminary experimental investigation no distinct parameters were chosen to be experimentally analyzed in detail. The principal parameters measured consisted of those required by the shock pulse diagnostic technique (p_1, p_2, U) and those amenable to

* More recent tests with 0.020 inch thick ablative coatings have been shown to more closely simulate the flush-mounted performance.

streak photographic measurement (v_1, v_2, U). Other measurements necessary included: flow rates and various temperatures and pressures. Among the most sensitive variables in the shock pulse analysis is the static pressure decay with axial location within the combustor. This meant that detailed static pressure surveys had to be made. This was accomplished with a mercury manometer, referenced to the injector end static pressure.

As stated previously, the experimental rocket motor was maintained at a length of 70 inches for these tests and was operated at a total flow rate of LOX/ALC of approximately 3#/sec. A nozzle was then chosen which set the chamber pressure at about 300 psia. Momentary operation above this pressure results from the fact that the chamber pressure rises to about twice its initial value following the pulse of the step pulse generator (double instantaneous flow rate). The chamber was operated at a mixture ratio which insures stable operation except when the motor was pulsed ($r = 2.3$).

These preliminary test runs were made with run durations of about 1.5 seconds, and did not use automatic shutdown. This test procedure consisted of a preflow of liquid oxygen to chill the lines and to insure that only LOX would reach the rocket injector. Then with the LOX flowing, gaseous oxygen and hydrogen were fed into the chamber and ignited with a spark plug. When the operator got a visual indication of ignition the fuel flow was switched on. This led to full combustion. Following this, the step pulse generator or pulse gun was discharged to initiate the first shock and subsequent instability. The run was then shut down. At approximately 10 seconds before the run was started the streak camera drive motor was started, this allowed sufficient time for the film to attain a constant speed before the shutter was opened. To insure that the first shock was contained on the streak film the shutter was synchronized with the pulse. This was easily accomplished by actuating the shutter with a 24 V DC solenoid, this voltage being the same as needed to initiate the pulse gun or step pulse generator. This synchronization allows part of the film to be exposed to the steady-state portion of the run and the remainder to the initial shock and its subsequent reflections. As in the cold flow study the shutter was set so as to expose most of the 80-inch film loop (shutter speed $\sim 1/25$ sec. for $v_f = 125$ ft/sec). During the test runs the output from the pressure

transducers was recorded on tape moving at high speed. Other electrical data (flow rate, temperatures, etc.) were stored on strip chart recorders.

Data Reduction

Since this discussion is concerned with the initiation of an experimental program to be used in conjunction with the shock pulse technique the data reduction is principally contained in the solution of the conservation equations (see Reference 4). The experimental study will merely supply inputs to the computer solution of these equations. Thus the data reduction involved with the shock pulse technique will not be discussed here. A discussion of this can be found in Reference 4. However, some discussion of the experimentally determined inputs to this technique is warranted, as well as a discussion of the other uses of the experimental data.

As previously discussed, several variables may be experimentally determined so that the conservation equations are determinate. These include the measurement of static pressure before and behind the shock velocity by means of high frequency response transducers and the measurement of gas velocity before and behind the shock by means of a streak camera. The modifications to the experimental research to permit these measurements have been nearly completed and data is expected in the near future. Prior to acquisition of this data several tests have been made with the formerly used transducers (Dynisco) and tape recorder (Ampex). This limited the frequency response but at least allowed the initial checkout of the pulse technique and computer solutions. These initial computer results can be found in Reference 4. These initial test runs also served to check out the photographic instrumentation (streak camera). The data obtained from streak photographs can serve as another input for the pulse technique, but it is primarily used for qualitative descriptions of the combustion processes and for measurements of c^* from the chamber gas velocity.

The input to the shock pulse technique from the pressure transducer data consisted of the static pressure immediately before and after passage of the shock and of the shock velocity. The pressure measurements

are relatively straight-forward, however, the shock velocity determination involved the use of the time differential between two transducers a known distance apart. This technique was beset with difficulties in the accurate measurement of the velocity due to the random time differences in the various channels of the 10 KHz tape recorder. This was one of the prime reasons which necessitated an upgraded recorder. Even so, these initial runs were made using the 10 KHz equipment in order to obtain preliminary data. In addition to use in the computer solution to the pulse techniques, the pressure data was used in a correlation with the streak velocity data to be described later.

The analysis of the streak film data was made with several intentions in mind. The principal intent was to reveal the usefulness of streak photography as an experimental tool, both for quantitative and qualitative results. The streak film was used to quantitatively obtain velocity data at various locations within the chamber and was used for qualitative examination of the combustion flow field (i.e., variations in luminosity and color).

The streak velocity data consisted primarily of the gas velocity* within the chamber. Other velocities measured included the shock velocity and the gas velocity immediately behind the shock. The initial use of the measured steady-state gas velocity was in the calculation of the characteristic exhaust velocity as outlined in Appendix B. In Fig. 17 can be seen the c^* vs. L curve for this research motor as obtained in the conventional way. The data points in this figure were obtained from the various streak velocity data values and the use of Fig. 21. The close agreement between the two methods points out the possibility of the use of streak photography for this measurement. When one considers the complexity of the conventional c^* vs. L measurements the use of streak velocity data becomes quite desirable since it is relatively simple to build a windowed research motor as opposed to a motor capable of operation with the nozzle placed at various distances from the injector. The agreement of this data also serves to illustrate that the conditions within this research motor are nearly one-dimensional, since the $c^* - v_g$ correspondence assumes one-dimensionality.

* At present it is not precisely known that the velocity measured is the gas velocity because of a variation in the velocities measured, but this velocity will be referred to as the gas velocity.

The next use of the streak film data also involves the pressure data as needed for the shock pulse technique. From this pressure data the pressure ratio across the initial shock and the shock velocity were obtained (Fig. 14). In the streak film data the velocity ratio across the shock and the shock velocity were determined (Fig. 17). Now if one uses the velocity ratio data the pressure ratio can be determined using the normal shock relations. When this is done the two independent measurements of the pressure ratio are found to agree within 5%. This agreement again illustrates the versatility of streak photographic data, but more importantly it might imply that the situation within the research rocket motor is not too far removed from the ideal conditions assumed for the normal shock relationships. Before it could be conclusively stated that the two situations are not too different, data on the temperature and density ratios would also be needed since these would probably be more sensitive to combustion than would the pressure ratio.

The next use of the streak data was to determine the speed of sound (temperature) distribution within the combustion chamber. This was easily accomplished from the measured gas and shock velocity through the velocity (or pressure) ratio across the shock. The shock Mach number was determined and hence the speed of sound was easily found. All of these data can be seen in Figure 18.

Before proceeding to the qualitative observations, a discussion of the previously determined steady-state velocity variations³⁶ is warranted. The Rocketdyne investigation has also found a variation, about 20%, in the measured streak velocities. Originally this variation was thought to be the result of droplet velocity measurements for the lower values and gas velocity for the higher. Recent studies^{37,31} have cast some doubt upon this interpretation and have led to some different interpretations,* the principal one being that the variations are due to concentration striations in the gaseous products (see Appendix B). Such concentration striations mean regions of non-nominal mixture ratio and hence different combustion temperatures and luminosities. The present investigation tends to confirm this interpretation rather than the boundary layer interpretation also proposed. Boundary layer

* Also see page 40.

effects should not be present in this case since the camera was focused on the motor centerline and the depth of field was short enough to keep the boundary layer outside the field of focus. Definite luminosity variations can be seen in all streak films, especially the few color films taken.

In addition to the quantitative use of the streak photography technique, several interesting qualitative observations can be seen in the streak photographs. In this investigation, most of the streak records were made using black and white film (Kodak Recording 2475). Such film was found to be easily exposed to the combustion light and to give good quantitative velocity results, however, its qualitative results leave something to be desired. For qualitative results of luminosity variations color film is recommended. This was used in several tests at the end of this investigation to determine its usefulness. Kodak Ektachrome was found to be fast enough for proper exposure and to yield good results.

In both the black and white and color streak films a pronounced effect of the initial shock can be seen (Fig. 19). It is easily seen that the shock is sufficiently strong to temporarily stop the gas flow and in some cases reverse it. But also significant changes in the luminosity of various regions can be seen. Following the passage of the first shock and its reflections is a region of very low luminosity, near the midpoint of the slit. This persists for several cycles of the pulse produced instability and moves toward the injector. After this the region disappears, and all subsequent cycles are quite similar. One explanation of this stationary region is that a cool stagnant region exists within the slit, which is opaque to luminosity within the chamber. However, this is only speculation and future testing may clarify this point.

With regard to the qualitative effects of the shock waves upon combustion, the color streak photographs seem to provide the best data. In these a slight increase in luminosity can be seen after passage of the first shock. It appears that the passage of the reflected shock has a greater effect upon combustion since a much larger increase in luminosity is observed after the reflected shock passes the window. With all of the instability cycles it appears that the downstream moving shock produces a greater effect upon combustion than does the upstream moving shock. Also

with suitable refinements in the photographic technique the possibility exists for rough determinations of mixture ratio from the various colors observed.

Results and Conclusions

The techniques discussed here are now being employed in the completely instrumented chamber. The results of those experiments will be subject for a subsequent technical report.

The principal results from this preliminary investigation are those obtained from the streak film analysis. These include quantitative results concerning the c^* distribution in the rocket motor and velocity results which seem to indicate a close degree of similarity of the research motor to a one-dimensional model. Perhaps of more basic importance to the study of the combustion processes within the chamber are the qualitative results of the streak films. Among these is one which has bearing on the interpretation of the cause of the variation in steady-state streak velocity measurements. It appears from variations in luminosity that the principal cause of the velocity variations is the presence of regions of different combustion concentrations which result from regions of nonuniform mixture ratio. This explanation seems more realistic than the previously espoused interpretation that droplet velocities represented the lower velocity limit and the gas velocity the upper limit.³⁶ If this were so the velocity variation should decrease at regions where the combustion is nearly complete. Research with gaseous propellants also exhibited this variation,³⁷ thus removing this interpretation as the only means available for such a variation. Other researchers⁴⁶ have proposed the concentration striation interpretation as an alternative and this author feels that this is more likely the proper interpretation.

The streak films also reveal some qualitative results concerning the effects of shock waves on combustion in the rocket motor. These include the observation that greater increases in luminosity are seen to occur after passage of the downstream moving shock rather than after the upstream moving shock. Since for the locations used in these tests the flow essentially returns to the steady-state velocity just prior to passage of the upstream moving shock, it may be postulated that the shock acts merely to more thoroughly mix the concentration striations previously discussed. It is felt that

only a small increase in burning occurs after passage of the upstream moving shock but that the downstream moving shock may cause a more pronounced effect since its temperature rise is building upon that of the initial shock. If this explanation is correct it should be capable of verification through the examination of streak films taken at locations far from the regions of primary combustion. In these preliminary studies this was done only to the extent of one streak film taken 29" from the injector, hence no conclusions can be drawn at this time. Another possible explanation is that the temperature rise of the reflected shock builds upon that of the upstream moving one and hence gives a higher local temperature after its passage than does the initial shock. This increased temperature may lead to the excitation of some combustion products and hence an increase in luminosity.

There can be no doubt as to the value of the quantitative results obtained from both the pressure and velocity measurements. The shock pulse technique should provide a basic insight into steady combustion processes, while the results of streak velocity data give good preliminary results concerning the axial combustion distribution within the chamber. Perhaps with streak cameras having a smaller depth of field transverse distributions could even be observed.

The experimental test program is now at the stage where useful results will soon be forthcoming. The analytical pulse technique is being provided with accurate experimental inputs and the streak photography technique is now operating without difficulties. Perfection of color streak photography will be emphasized for the future.

APPENDIX A: TECHNIQUES OF STREAK PHOTOGRAPHY

The domain of streak photography as a valuable experimental technique is reached when one wishes to obtain an accurate description of an object's motion in the coordinates of position and time. This technique is desirable in many combustion, gas dynamic, and engineering research areas. Such information is of course obtainable from high speed motion pictures, but only after laborious transformation of many still pictures into a quantitative displacement curve. The method of streak photography directly results in a Cartesian coordinate plot of the displacement - time history of an object's motion within the field of view. Thus, streak photography possesses a great advantage over high speed pictures by the elimination of point by point plotting when displacement curves are desired. An additional advantage of streak techniques is that of greater accuracy, due to the elimination of frame-by-frame measurements. In general the methods of streak photography are easily performed by a wide variety of optical arrangements and quantitative results can be obtained with relatively inexpensive equipment.

The basic, underlying principle of streak photography involves the differential motion between the radiation sensitive material and the incident radiation, and thus the technique is non-image-forming (i.e. a blurred photographic image is recorded). In practice an object moving perpendicular to a moving piece of film supplies the differential motion required for streak photography. The film may be either in motion or stationary with the apparent film motion in the latter case being supplied by a rotating mirror. For extremely fast apparent film speeds both moving film and a rotating mirror may be used. The basic optical arrangement consists of a light source, lens and slit as is shown schematically in Figure 20.

The accuracy of a streak camera is ordinarily expressed in terms of both space and time. Spatial resolution is determined by the maximum number of equally spaced lines per mm. that can be distinguished in the photographic image and is found by photographing test patterns with various line spacings. Time resolution is similarly defined as the minimum time interval that is distinguished in the displacement-time record.

Thus, the time resolution of a motion picture camera is simply the time interval between two adjacent frames. On the other hand, several factors determine the time resolution of a streak camera. These include: 1) film velocity, 2) effective slit width, and 3) spatial resolving power of the recording medium. For high time resolution one uses a narrow slit in combination with a fast film velocity and large resolving power. The upper limit of time resolution is expressed as the reciprocal of the product of the spatial resolving power and the film velocity past the slit. Thus with a film velocity of .04 mm/ μ sec (130 ft/sec) and a spatial resolving power of 10 lines/mm the limiting time resolution of the system is $\frac{1}{10} \times \frac{1}{.04} = 2.5 \mu$ sec.

Incorporation of the slit into the optics system of a streak camera can be obtained through various techniques, of which the following are examples: 1) the slit is placed in the object plane; 2) the slit is placed in the focal plane of the primary objective lens and a secondary optical system is then used to refocus both the slit and primary image onto the film; 3) the slit is placed near the film surface; and 4) no physical slit is required if the object consists of a spot or narrow band of light. Also systems have been devised to obtain various results which incorporate the use of multiple slits.^{18,19} These may be either parallel or crossed and continuous or discontinuous depending upon the desired results.

There are two distinct classes of streak camera: 1) those using a limited length of film and 2) those using long lengths of film. The first class consists of drum, spinning-mirror, and continuous loop camera, which can be brought up to, and maintained at, a constant speed before the pertinent event is recorded. This feature has the advantage of providing a uniform time scale while eliminating excessive waste of film. However, duration of the exposure is limited, and hence only short duration events can be entirely recorded. Another problem may be the synchronization of camera shutter with the event. The second class of streak cameras is commonly referred to as a strip camera. For operation at high speed, strip cameras may not reach a constant film velocity before the film is expended, but they have the advantage of being able to record relatively long events on one film with relatively minor problems of synchronization.

However, for quantitative work an accurate scale must be placed on the film since it is not at constant speed. Also, since in many applications those events recorded at the film's initial slow speed are of little value, much film and developing time may be wasted.

In addition to the advantages of a continuous time-displacement record, a streak camera, operating at the same film velocity as a framing camera, is capable of recording frequencies and subject velocities several orders of magnitude higher than can be recorded with a framing camera or conversely the streak film velocity required to record rapidly moving objects is considerably less than that required for a framing camera.¹⁷

One prime disadvantage of streak photography is its limitation to linear motions that are perpendicular to the direction of film motion. Small motions of the object parallel to the film motion can result in appreciable errors. However, a modified streak photographic technique has been devised²⁰ to eliminate this error and permit the application of streak photography to some of those cases not applicable to ordinary streak photography. Basically this method makes use of a small rigid body attached to the object whose motion is being studied. On this body are scribed parallel lines which are perpendicular to the principle component of motion. The image of these lines is approximately a point on the film and any displacement of the object parallel to the film will not result in any displacement of the image on the film. However, this technique is only applicable to the motion study of solid objects and hence has little value to research in combustion and/or gas dynamics.

The primary mode of operation of streak cameras is in the measurement of velocity. This is accomplished by orienting the camera such that the slit is parallel to the direction of motion, the optical axis is normal to this direction and of course the film velocity vector is normal to the slit. A schematic of this operational setup is shown in Figure 20. As can be readily verified by simple geometric and trigonometric arguments, the velocity to be measured is a function of the film velocity, optical magnification, and the streak angle. This relation is in fact: $v = v_f \tan \gamma / M$.

There is no limitation placed upon streak photography by the type of optical system desired. This experimental technique is amenable

to all optical systems, from direct photography to color schlieren or interferometry.¹⁸ However, to date the principal optical systems used in combustion and/or gas dynamics research have been shadowgraph and schlieren.²¹⁻²⁵ Shadowgraph techniques have been used in many shock and detonation studies with excellent results, however, for extremely weak disturbances schlieren systems provide an even better approach. Light-reflection systems of direct photography have found their primary application to projectile motion and mechanical vibration studies.²⁰ Streak photographic techniques have also been applied to the self-luminous events associated with detonation studies and rocket combustion processes.²⁷⁻³⁴ The work by Berman et al²⁷⁻²⁹ was the first major use of streak photography in liquid rocket research and established it as a useful experimental technique for such research, especially in the area of combustion instability (for further details see Appendix B). Some work has been done with shadow techniques^{32,35-37} but due to the intense combustion light only very powerful backlights may be used unless a two-dimensional motor is provided to keep the chamber thin and thereby improve backlight penetration. In addition to these relatively straight-forward optical systems, more sophisticated techniques have been used in conjunction with streak photography. These include streak spectrography and streak interferometry. Conversion of a streak camera into a spectrograph is readily accomplished by placing a prism or transmission grating before the camera lens and using the camera slit as the spectrograph slit. In principle these time dependent spectra can be converted into a temperature-time history. Streak interferometry has found some applications in the study of exploding wires and should be applicable to other transient phenomena. Bennett, Sheen and Burden³⁸ describe this new technique in some detail. Finally, the application of color film can greatly increase the versatility of all of these techniques.

From the above discussion we can see that streak photography techniques are suitable in a wide variety of applications and will yield excellent quantitative and qualitative results.

The references cited in this appendix and subsequent references listed by these researchers can be used to obtain much more detail on the streak photography technique than that which has been provided here.

APPENDIX B:

APPLICATION OF STREAK PHOTOGRAPHY TO ROCKET COMBUSTION STUDIES

Research in the field of liquid rocket combustion processes is an area which is more than amply supplied with experimental difficulties. These difficulties have impeded the collection of experimental evidence to support simplified theoretical models of combustion in liquid propellant rockets. It is not difficult to understand the reasons for the experimental problems. One only has to look at the high pressure, high temperature environment that one finds within a rocket combustion chamber. Coupled with this uninviting environment are the rather complex and detailed combustion properties which one would need to know to describe in quantitative detail, the combustion processes. Among these properties are: the propellant spray geometry, the spatial disintegration rates of the propellant streams, the sizes and numbers of droplets in the propellant spray, the droplet vaporization rates, the velocities of burning droplets and gaseous combustion products, the resulting axial and/or tangential combustion distribution, etc. These parameters can be measured under atmospheric conditions and modest temperatures, but under the conditions found in rocket chambers few experimental techniques remain useful. Those remaining useful include water cooled mechanical probes,³⁹ acoustic measurements,⁴⁰ and photographic techniques. This discussion will describe the application of streak photography to combustion process research, specifically concerning investigations of combustion instability and performance measurements.

Of course the application of streak photography to rocket combustion research is concerned with the quantitative measurement of velocities within the chamber and with qualitative results from luminosity variations. Many applications make use of the combustion radiation rather than using a high intensity backlighting source.^{35,36,41} To date most streak photographic research on rocket motors has been done with either full-length windows in the motor or a transparent motor. The latter setup naturally requires very short testing time and frequent replacement of the chamber. However, it does allow the whole combustion chamber to be viewed, whereas a window in a metallic motor restricts the field of view while

permitting longer run times and eliminating the need for frequent window replacements. Since it is desirable to obtain information along the entire chamber length, most applications have windows for the entire length. This, however, means that the resulting image size will be very small (a magnification factor much less than 1) if the entire chamber is to be photographed at once.

The commonly used performance parameter of rocket engines is the characteristic exhaust velocity, c^* . This parameter is a measure of the fraction of theoretical combustion which has taken place. Normally c^* is experimentally determined by measuring the propellant flow rate and chamber pressure, $c^* = \frac{P_c A_t g}{\dot{w}}$. As will be shown the characteristic velocity can also be related to the axial gas velocity. This relation is primarily dependent on chamber geometry, while being relatively insensitive to combustion properties and independent of the propellant flow rate and chamber pressure. Thus c^* can be measured by this method which is entirely independent of the conventional set of measurements. Streak photography is one photographic technique readily suited for the measurement of the axial gas velocity, and the axial variation of velocity is easily obtained. In fact, as will be discussed later, the streak films yield a range of velocities at any axial location.^{36,44} These have been thought to be gas velocity at the upper limit and droplet velocities at the lower limit, however, other data has tended to place this interpretation somewhat in question.^{37,41}

Assuming constant, one-dimensional, gaseous flow with no heat addition in the converging portion of the nozzle, one can derive the relation between chamber gas velocity and the characteristic velocity.⁴²

The dynamic pressure is given by,

$$q_c(x) = \frac{1}{2} \frac{\rho_c(x) v_c^2(x)}{g} \quad (B-1)$$

for a compressible gas at Mach number below 2.0,

$$\frac{P_c(x) - p_c(x)}{q_c(x)} = 1 - \frac{M_c^2(x)}{4} \quad (B-2)$$

Using Equation (B-1) and the continuity equation $\dot{w} = \rho_c(x) A_c v_c(x)$ Equation (B-2) can be written,

$$P_c(x) = P_c(x) - \frac{\dot{w} v_c(x)}{Z A_c g} \left(1 - \frac{M_c^2(x)}{4}\right) \quad (B-3)$$

For a perfect gas this becomes,

$$\frac{t_c(x)}{m_c} = \frac{P_c(x)}{\rho_c(x) R} = \frac{P_c(x) A_c v_c(x)}{\dot{w} R} - \frac{v_c^2(x)}{Z R g} \left(1 - \frac{M_c^2(x)}{4}\right) \quad (B-4)$$

The fundamental equation for the characteristic velocity is,

$$C^*(x) = \frac{\sqrt{\gamma g R \frac{T_c(x)}{m_c}}}{\gamma \left(\frac{2}{\gamma+1}\right)^{\frac{\gamma+1}{2(\gamma-1)}}} \quad (B-5)$$

which may be written,

$$\frac{T_c(x)}{m_c} = \gamma \left(\frac{2}{\gamma+1}\right)^{\frac{\gamma+1}{\gamma-1}} \frac{C^{*2}(x)}{g R} \quad (B-6)$$

From the isentropic flow relation,

$$\frac{T_c(x)}{t_c(x)} = 1 + \frac{\gamma-1}{2} M_c^2(x)$$

Thus,

$$\frac{t_c(x)}{m_c} = \frac{\gamma \left(\frac{2}{\gamma+1}\right)^{\frac{\gamma+1}{\gamma-1}} C^{*2}(x)}{\left(1 + \frac{\gamma-1}{2} M_c^2(x)\right) g R} \quad (B-7)$$

Equating Equations (B-4) and (B-7) and simplifying by using the definition,

$$C^*(x) = \frac{P_c(x) A_t(x) g}{\dot{w}} \quad \text{one obtains,}$$

$$\gamma \left(\frac{2}{\gamma+1}\right)^{\frac{\gamma+1}{\gamma-1}} C^{*2}(x) = \frac{A_c}{A_t(x)} v_c(x) \left(1 + \frac{\gamma-1}{2} M_c^2(x)\right) C^*(x) - \frac{v_c^2(x)}{Z} \left(1 + \frac{\gamma-1}{2} M_c^2(x)\right) \left(1 - \frac{M_c^2(x)}{4}\right) \quad (B-8)$$

for $M_c(x) \leq .3$ this reduces to,

$$\gamma \left(\frac{2}{\gamma+1} \right)^{\frac{\gamma+1}{\gamma-1}} C^*(x) = \frac{A_c}{A_t(x)} v_c(x) C^*(x) - \frac{v_c^2(x)}{2} \quad (B-9)$$

The throat area is written as a function of x because the throat is essentially being placed at various axial locations with different conditions at the nozzle inlet and hence it must change to pass the same flow rate.

For the derivation of $A_t(x)$ the assumption of constant flow rate is again made.

$$\rho_t(x) A_t(x) v_t(x) = \rho_t(L) A_t(L) v_t(L)$$

or

$$\frac{A_t(x)}{A_t(L)} = \frac{\rho_t(L) v_t(L)}{\rho_t(x) v_t(x)} \quad (B-10)$$

but

$$\frac{v_t(L)}{v_t(x)} = \left[\frac{t_t(L)}{t_t(x)} \right]^{1/2} = \left[\frac{T_t(L)}{T_t(x)} \right]^{1/2}$$

also,

$$\frac{\rho_t(L)}{\rho_t(x)} = \frac{\rho_{ot}(L)}{\rho_{ot}(x)}$$

therefore,

$$\frac{A_t(x)}{A_t(L)} = \frac{\rho_{ot}(L)}{\rho_{ot}(x)} \left[\frac{T_t(L)}{T_t(x)} \right]^{1/2} \quad (B-11)$$

but,

$$\rho_o(x) = \left(1 + \frac{\gamma-1}{2} M_c^2(x) \right)^{\frac{1}{\gamma-1}} \rho_c(x) = \rho_{ot}(x)$$

and,

$$T(x) = \left(1 + \frac{\gamma-1}{2} M_c^2(x) \right) t_c(x) = T_t(x)$$

thus,

$$\frac{A_t(x)}{A_t(L)} = \left[\frac{1 + \frac{\gamma-1}{2} M_c^2(L)}{1 + \frac{\gamma-1}{2} M_c^2(x)} \right]^{\frac{\gamma+1}{2(\gamma-1)}} \frac{\rho_c(L)}{\rho_c(x)} \left[\frac{t_c(L)}{t_c(x)} \right]^{1/2} \quad (B-12)$$

from continuity,
$$\frac{\rho_c(L)}{\rho_c(x)} = \frac{v_c(x)}{v_c(L)}$$

and also,
$$\left[\frac{t_c(L)}{t_c(x)} \right]^{1/2} = \left[\frac{1 + \gamma M_c^2(x)}{1 + \gamma M_c^2(L)} \right] \left[\frac{v_c(L)}{v_c(x)} \right]^{1/2}$$

therefore,
$$\frac{A_t(x)}{A_t(L)} = \left[\frac{1 + \frac{\gamma-1}{2} M_c^2(L)}{1 + \frac{\gamma-1}{2} M_c^2(x)} \right]^{\frac{\gamma+1}{2(\gamma-1)}} \left[\frac{1 + \gamma M_c^2(x)}{1 + \gamma M_c^2(L)} \right]^{1/2} \left[\frac{v_c(x)}{v_c(L)} \right]^{1/2} \quad (B-13)$$

For the case of $\gamma = 5/4$ and $M_c(L) = .3$, $M_c(x) = 0$, which is the most extreme case,
$$\frac{A_t(x)}{A_t(L)} = .997 \left(\frac{v_c(x)}{v_c(L)} \right)^{1/2} \quad (B-14)$$

thus,
$$\frac{A_t(x)}{A_t(L)} \approx \left[\frac{v_c(x)}{v_c(L)} \right]^{1/2}$$

or
$$\frac{A_t(x)}{v_c(x)} = A_t(L) \frac{1}{\sqrt{v_c(L) v_c(x)}} \quad (B-15)$$

Finally substituting this result into Equation (B-9), one obtains,

$$\gamma \left(\frac{2}{\gamma+1} \right)^{\frac{\gamma+1}{\gamma-1}} C^{*2}(x) = \frac{A_c}{A_t(L)} \sqrt{v_c(L) v_c(x)} C^{*}(x) - \frac{v_c^2(x)}{2} \quad (B-16)$$

Thus, we have obtained the characteristic velocity as a function of only the contraction ratio, ratio of specific heats, and the gas velocity. Equation (B-16) can be seen plotted in Figure 21.

As can be seen from Equation (B-15) the characteristic velocity

is proportional to the square root of the gas velocity. Had we not assumed that the mass flow was all gas and constant, but that our gas mass flow was increasing as liquid was vaporized, the characteristic velocity would have been linear with the gas velocity for the limiting case of constant temperature.

This technique will certainly never replace the normally used method of evaluating the overall rocket combustion performance parameter, c^* , because of the greater experimental difficulty and larger errors. These errors arise from several factors, the principal ones being the non one-dimensionality of the flow and the spread in velocities measured. A streak camera is inherently limited to studies of one-dimensional phenomena and therefore the streak velocity measurements in regions which are not one-dimensional (i.e., near the injector) can not be considered to be accurate. The second error involved with this technique arises from the spread in velocities measured.^{36,41,44}

The original thought was that the highest streak velocities correspond to the combustion gas velocity while the lower streak velocities represent the velocities of burning droplets.³⁶ However more recent results using gaseous propellants³⁷ have shown similar velocity boundaries. Thus several other physical explanations of the lower velocity boundary have been proposed. These include: combustion gas turbulence, boundary layer effects, concentration striations in the combustion gas stream and condensation of water vapor near the injector. Of these, the explanation by concentration striations seems the most plausible. Turbulent velocity fluctuations about some mean value does not explain the fact that the upper boundary closely approximates the gas velocity as calculated from one-dimensional theory. References 37 and 41 have shown that boundary layer effects do not seem to explain the variation. Water vapor condensation has been observed in some tests but not in others³⁷ and hence this explanation also fails to fully explain the measured velocity envelope. Reference 41 also found evidence of variations of radiation intensity within the motor which could correspond to concentration striations and hence explain the velocity envelope. However, even with the lower boundary of the velocity envelope still in doubt, the upper boundary or combustion gas velocity profile can still be used to obtain useful comparisons and conclusions.

By itself the characteristic velocity is, however, of little use in the detailed description of combustion processes. This is where streak photography can supply more localized information pertaining to gas velocities, droplet velocities and accelerations, and general changes in luminosity. One great advantage which the streak photographic technique does possess over the normally used method of c^* calculation is that the c^* vs. L curve can be obtained at once while the other method necessitates making several measurements with the nozzle placed at various distances from the injector.

Perhaps the primary use of c^* vs. L data is in the determination of distribution of propellant vaporization^{45,46} or combustion.

The theoretical value of c^* is given by:

$$\frac{P_c A_{tg}}{\dot{w}_g} = \frac{P_c A_{tg}}{\chi_\phi \dot{w}_\phi + \chi_F \dot{w}_F} \quad (B-17)$$

While the experimentally determined value is simply,

$$C_{EXP}^* = \frac{P_c A_{tg}}{\dot{w}} = \frac{P_c A_{tg}}{\dot{w}_F + \dot{w}_\phi} = \frac{P_c A_{tg}}{\dot{w}_g + \dot{w}_F} \quad (B-18)$$

Combining (B-17) and (B-18) gives

$$C_{EXP}^* = C_{th}^* \left(\frac{\dot{w}_g}{\dot{w}} \right) = C_{th}^* \frac{\chi_\phi \dot{w}_\phi + \chi_F \dot{w}_F}{\dot{w} + \dot{w}_F} \quad (B-19)$$

Now defining the c^* efficiency, η_{c^*} , as

$$\eta_{c^*} = \frac{C_{EXP}^*}{C_{th}^*} = \frac{\dot{w}_g}{\dot{w}} = \frac{\chi_\phi \dot{w}_\phi + \chi_F \dot{w}_F}{\dot{w}_\phi + \dot{w}_F} \quad (B-20)$$

If one now assumes that one of the propellants is fully vaporized at the exhaust nozzle, the fraction vaporized of the other propellant can be obtained from η_{c^*}

For oxidant completely vaporized:

$$\eta_{c*} = \frac{C_{th}^* (1, \chi_F)}{C_{th}^*} \frac{\left(\frac{\dot{w}_o}{\dot{w}_F} + \chi_F\right)}{\left(\frac{\dot{w}_o}{\dot{w}_F} + 1\right)} \quad (B-21)$$

and with fuel completely vaporized:

$$\eta_{c*} = \frac{C_{th}^* (\chi_o, 1)}{C_{th}^*} \frac{\left(\frac{\chi_o \dot{w}_o}{\dot{w}_F} + 1\right)}{\left(\frac{\dot{w}_o}{\dot{w}_F} + 1\right)} \quad (B-22)$$

This data can also be used in conjunction with the pulse technique described in part II.

Here we have:

$$\frac{C_{exp}^*}{C_{th}^*} = \frac{\dot{w}_g}{\dot{w}} = \frac{\rho_g A_c v_g}{\dot{w}} \quad (B-23)$$

thus:

$$\rho_g v_g = \frac{C_{exp}^*}{C_{th}^*} \frac{\dot{w}}{A_c} \quad (B-24)$$

and also:

$$\frac{C_{exp}^*}{C_{th}^*} = 1 - \frac{\dot{w}_g}{\dot{w}} = 1 - \frac{\rho_g v_g A_c}{\dot{w}} \quad (B-25)$$

where ρ_g is a bulk density.

Thus

$$\rho_g v_g = \frac{\dot{w}}{A_c} \left(1 - \frac{C_{exp}^*}{C_{th}^*}\right) = \frac{\dot{w}}{A_c} - \rho_g v_g \quad (B-26)$$

If we now measure v_g or v_g with a streak camera the bulk densities ρ_g and ρ_g can be determined and used in the pulse technique.

Thus we see that streak photography has a very useful application to the experimental study of liquid rocket steady-state combustion processes. Of equal importance to its semi-quantitative use described here, is its application as a technique for qualitative studies of combustion processes.

Still another area of liquid rocket combustion research has made use of streak photography, this is the study of transient phenomena, specifically combustion instability. The leader in the development and a use of this technique was Berman²⁷⁻²⁹ at General Electric. His research concerned longitudinal pressure oscillations and was instrumental in revealing this technique as a promising method for the determination of gas and particle velocities in an unstable rocket engine. Subsequently, investigations of tangential instability were also performed using this technique.³⁴ More recently streak photography has been applied to the study of transverse instability in a two-dimensional research motor.^{41,43} Streak photographic techniques have also been applied to this same motor for studies of droplet and gas velocities.

The principal quantitative application of streak photography has been the determination of the time dependent pressure profiles within the unstable combustor from the velocity profiles as seen on the streak photographs. Assuming nonviscous flow one can obtain the axial gradient of the pressure from the momentum equation.

$$\frac{\partial v}{\partial t} + v \frac{\partial v}{\partial x} = - \frac{1}{\rho} \frac{\partial p}{\partial x} \quad (\text{B-27})$$

The time rate of change of pressure at any axial location can similarly be derived from the continuity equation.

$$v \frac{\partial \rho}{\partial p} \frac{\partial p}{\partial x} + \rho \frac{\partial v}{\partial x} = - \frac{\partial \rho}{\partial p} \frac{\partial p}{\partial t} \quad (\text{B-28})$$

Now the speed of sound is given by

$$a = \sqrt{\frac{\partial p}{\partial \rho}}$$

Using this and Equation (B-27), Equation (B-28) becomes

$$\frac{1}{\rho} \frac{\partial \rho}{\partial t} = v \frac{\partial v}{\partial t} - (a^2 - v^2) \frac{\partial v}{\partial x} \quad (\text{B-29})$$

From these relationships one can approximately determine the pressure gradients if the speed of sound and density are known and the velocity gradients (time and space) are measured. Using this procedure Berman²⁸ showed that the upstream moving shock is followed by a rarefaction.

Another quantity which can be determined from the velocity gradient across the shock is the pulse strength. This is accomplished by assuming the pressure pulse to be a steady one-dimensional normal shock with no heat release. One then gets for the pressure ratio

$$\frac{P_2}{P_1} = \frac{\frac{\gamma+1}{\gamma-1} \frac{v_{r1}^2}{a^{*2}} - 1}{\frac{\gamma+1}{\gamma-1} - \frac{v_{r1}^2}{a^{*2}}} \quad (\text{B-30})$$

where $a^{*2} = v_{r1} v_{r2}$

or

$$\frac{P_2}{P_1} = \frac{\frac{\gamma+1}{\gamma-1} \frac{v_{r1}}{v_{r2}} - 1}{\frac{\gamma+1}{\gamma-1} - \frac{v_{r1}}{v_{r2}}} \quad (\text{B-31})$$

and

$$\frac{P_2}{P_1} = \frac{v_1}{v_2} \quad (\text{B-32})$$

and

$$\frac{T_2}{T_1} = \frac{P_2}{P_1} \frac{v_2}{v_1} \quad (\text{B-33})$$

From this shock strength the shock Mach number can also be determined from one-dimensional gas dynamics and hence the speed of sound (or the gas temperature) is found from the measured value of the shock velocity.

Thus we see that for oscillations without strong shocks, streak photographic measurements of the gas velocities before and after the shock, and the shock velocity can yield the entire range flow field parameters within the limits of the one-dimensionality assumption. Also the measurement of shock velocities as the shock progresses through a previously undisturbed combustion zone should yield a profile of temperature along the combustor.

The two principal applications just discussed point out the usefulness of streak photography as a diagnostic technique in rocket combustion research. The use of high intensity light sources also contributes to the versatility of streak photography, particularly in the study of injection in liquid propellant rockets.^{35,36,41} This technique can be made very effective where an optical filter is used to block the combustion light but allows the backlight to pass. A commonly used high intensity light source makes use of mercury vapor radiation. In this case a 5470 Å filter excludes the combustion light and provides clear visualization of liquid streams and droplets.

REFERENCES

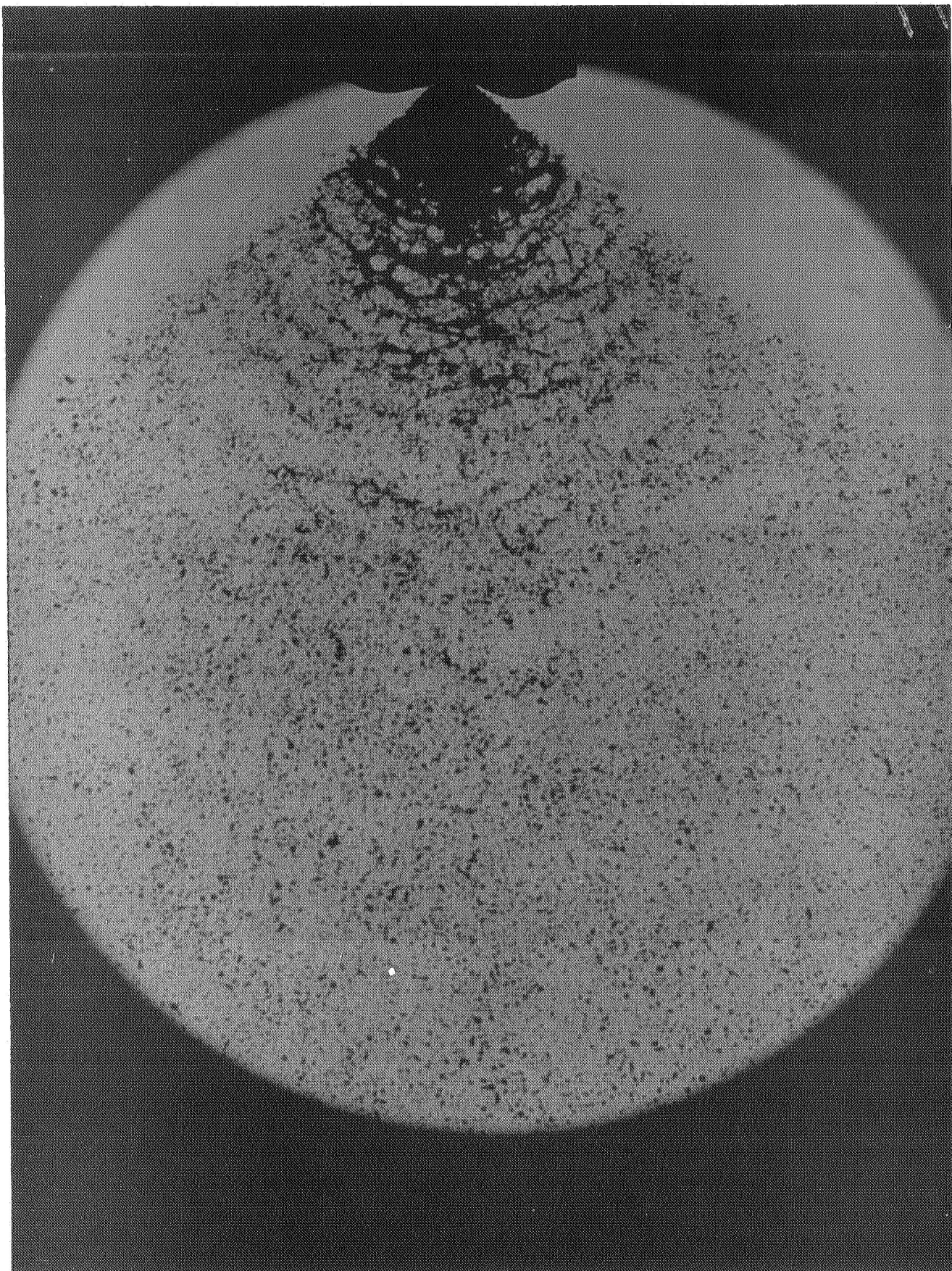
1. Gary, D.A., "A Study of Injector Spray Characteristics in a Simulated Rocket Combustion Chamber Including Longitudinal Mode Pressure Oscillations", Princeton University Department of Aerospace and Mechanical Sciences Technical Report No. 730, June 1966.
2. Crocco, L., Harrje, D.T., Sirignano, W.A., et al, "Nonlinear Aspects of Combustion Instability in Liquid Propellant Rocket Motors", Princeton University Department of Aerospace and Mechanical Sciences Report No. 553-e, 1965.
3. ibid, Report No. 553-f, 1966.
4. ibid, Report No. 553-g, 1967.
5. Heidmann, M.F., and Humphrey, J.C., "Fluctuations in a Spray Formed by Two Impinging Jets", Journal of the American Rocket Society (JARS), Vol. 22, No. 3, 1952.
6. Priem, R.J., Heidmann, M.F., and Humphrey, J.C., "A Study of Sprays Formed by Two Impinging Jets", NACA TN 3835, 1957.
7. Giffen, E. and Muraszew A., "The Atomization of Liquid Fuels", John Wiley and Sons, Inc. 1953.
8. Giffen, E. and Neale, M.C., "Affect of Gas Viscosity on Spray Atomization", The Motor Industry Research Association, Report No. 1954/4.
9. Giffen, E. and Lamb, T.A.J., "The Effect of Air Density on Spray Atomization", The Motor Industry Research Association, Report No. 1953/5.
10. Riebling, R.W. and Powell, W.B., "The Properties of Flowing Sheets Formed by Impingement of Liquid Jets on Curved Surfaces", AIAA preprint 66-610, 1966.
11. Combs, L.P., Hoehn, F.W., Webb, S.R., et al, "Combustion Stability Rating Techniques", AFRPL TR-66-229, 1966.
12. Brubaker, T., unpublished work at Princeton University, 1965.
13. Reba, I. and Coleman, B., "Combustion Instability: Liquid Stream and Droplet Behavior", Aeronautical Research Laboratories, Wright-Patterson AFB, WADC 59-720, 1960.
14. Cady, W.M., "Velocity Measurements by Illuminated or Luminous Particles", Vol. IX High Speed Aerodynamics and Jet Propulsion, Princeton University Press, 1954.
15. Diederichsen, J. and Wolfhard, H.G., "Spectrographic Examination of Gaseous Flames at High Pressure", Proceedings of the Royal Society (London), Vol. 236, No. 1204, July 10, 1956.

16. Wright, F.H., "The Particle-Track Method of Tracing Fluid Streamlines", JPL Progress Report No. 3-23, March 1951.
17. Hyzer, W.G., Engineering and High-Speed Photography, The MacMillan Company, 1962.
18. Liddiard, T.P., Jr. and Drimmer, B.E., "Smear-Camera Techniques", 5th International Congress on High-Speed Photography.
19. "The Use of the Rotating Drum Camera for the Measurement of the Velocities of Shell or Bomb Fragments", Office of Scientific Research and Development, OSRD 3900, July 15, 1944.
20. Vigness, I. and Nowak, R.C., "Streak Photography", Journal of Applied Physics, Vol. 21, May 1950.
21. Lewis, B. and Von Elbe, G., Combustion, Flames and Explosions of Gases, Academic Press, 1951.
22. Payman W. and Shepherd, W.C.F., "Explosion Waves and Shock Waves", Proceedings of the Royal Society (London), Vol. 186, No. 1006, Sept. 1946.
23. Fristrom, R.M. and Westenberg, A.A., Flame Structure, McGraw Hill, 1965.
24. Payman, W. and Titman, H., "Explosion Waves and Shock Waves", Proceedings of the Royal Society (London), Vol. A152, 1935.
25. Glass, I.I., Martin, W., and Patterson, G.P., "A Theoretical and Experimental Study of a Shock Tube", UTIA Report No. 2, November 1953.
26. Dabora, E.K., Ragland, K.W., Ranger, A.A. and Nicholls, J.A., "Two Phase Detonations and Drop Shattering Studies", NASA CR 72225, April 1967.
27. Berman, K. and Cheney, S.H., Jr., "Rocket Motor Instability Studies", JARS, Vol. 25, No. 10, October 1955.
28. Berman, K. and Cheney, S.H., Jr., "Combustion Studies in Rocket Motors", JARS, Vol. 23, No. 2, March 1953.
29. Berman, K. and Logan, S.E., "Combustion Studies with a Rocket Motor Having a Full-Length Observation Window", JARS, Vol. 22, No. 2, March 1952.
30. Altseimer, J.H., "Photographic Techniques Applied to Combustion Studies - Two-Dimensional Transparent Thrust Chamber", JARS, Vol. 22, No. 2, March 1952.
31. Barrere, et al, Rocket Propulsion, Elsevier Publishing Co., 1960.
32. Lawhead, R.B. and Combs, L.P., "Modeling Techniques for Liquid Propellant Rocket Combustion Processes", 9th Combustion Symposium.
33. Ingebo, R.D., "Heat Transfer and Drag Coefficients for Ethanol Drops in a Rocket Chamber Burning Ethanol and LOX", 8th Combustion Symposium.

34. Male, T., Kerslake, W.R., Tischler, A.O., "Photographic Studies of Rotary Screaming and Other Oscillations in a Rocket Engine", NACA RM E54A29, May 1954.
35. Rossman, T.G., Eulner, R.N., and Wood, L.M., "Photographic Investigation of Propellant Stream Behavior in a Firing Rocket Engine", Bell Aerosystems Report No. 9136-950001, Volumes I and II, June 1966.
36. Lambiris, S. and Combs, L.P., "Steady-State Combustion Measurements in a LOX/RP-1 Rocket Chamber and Related Spray Burning Analysis", Research Report RR-61-13, Rocketdyne, May 1961.
37. Combs, L.P. and Hoehn, F.W., "Steady-State Combustion of Gaseous Hydrogen and LOX", Research Report RR-64-24, Rocketdyne, June 1964.
38. Bennett, F.D., Shear, D.D., and Burden, H.S., "Streak Interferometry", Journal of the Optical Society of America, No. 50, No. 3, March 1960.
39. Trent, C.H., "An Investigation of Combustion in Rocket Thrust Chambers", Industrial and Engineering Chemistry, April 1956.
40. Hersch, M., "Determination of Local and Instantaneous Combustion Conditions from Acoustic Measurements in a Rocket Combustor and Comparison with Overall Performance", NASA TND-1192.
41. Kesselring, R.C., "Steady-State Streak Film Analysis in a High-Pressure, Two-Dimensional Research Motor", Rocketdyne, AIAA Paper No. 66-612, June 1966.
42. Heidmann, M.F. and Auble, C.M., "Rocket Performance Measurements with Streak Photographs", ARS Preprint 239-55.
43. Levine, R.S., Special Seminar at Princeton University, 1966.
44. Lambiris, S., Combs, L.P., and Levine, R.S., "Stable Combustion Processes in Liquid Propellant Rocket Engines", Rocketdyne, 5th Colloquium of the Combustion and Propulsion Panel, Advisory Group for Aeronautical Research and Development, NATO, Braunschweig, Germany, April 1962.
45. Clark, B.J., Hersch, M. and Priem, R.J., "Propellant Vaporization as a Criterion for Rocket Engine Design; Experimental Performance, Vaporization, and Heat Transfer Rates with Various Propellant Combinations", NASA Memo 12-29-58E.
46. Priem, R.J. and Heidmann, M.F., "Propellant Vaporization as a Design Criterion for Rocket Engine Combustion Chambers", NASA TR R-67.
47. Balling, N.R. and Connor, B.V., "An Electromagnetic Flowmeter for Low Conductivity Fluids", JPL Technical Report No. 32-329.

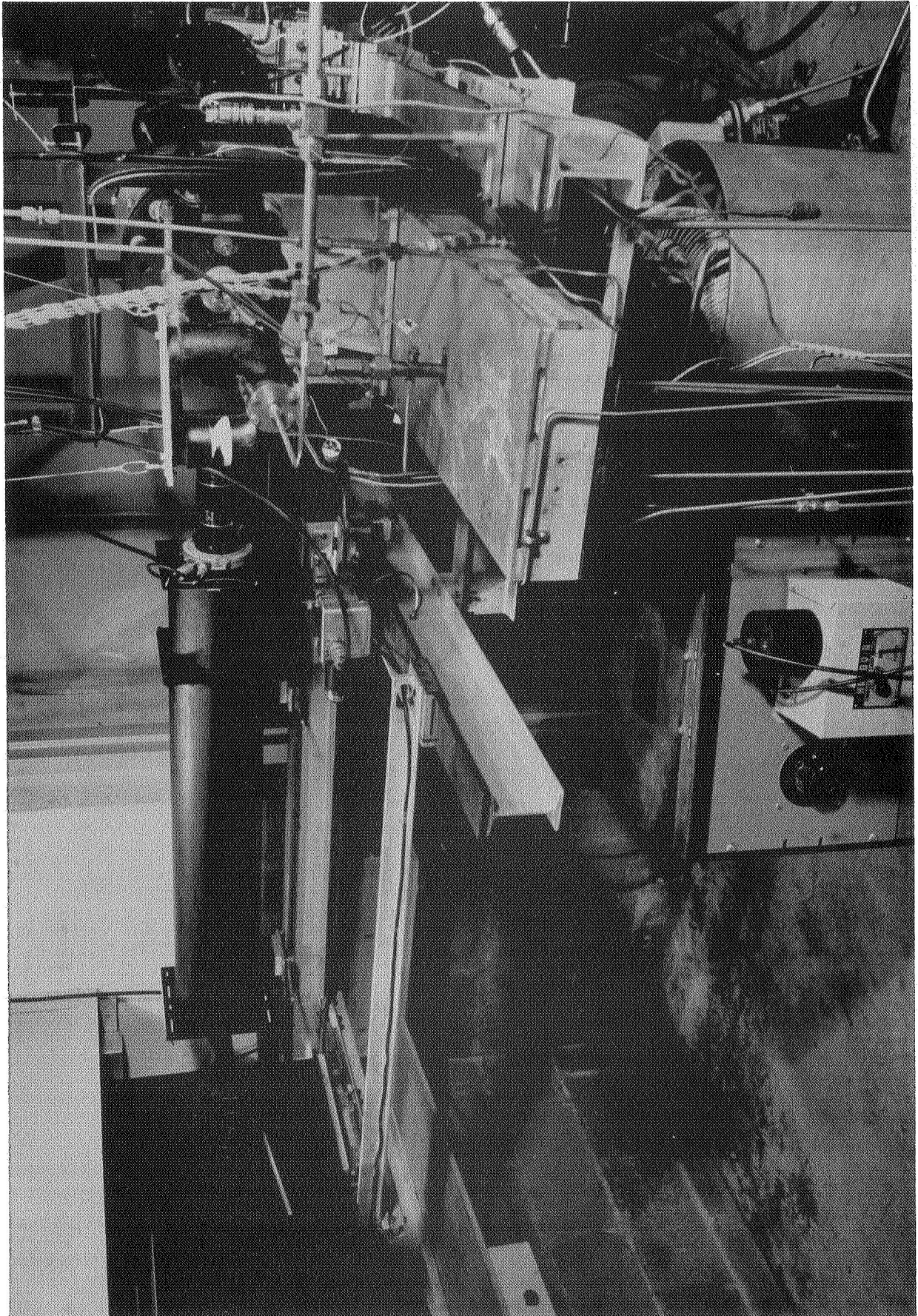
LIST OF FIGURES

1. Photograph of Typical Spray Pattern
2. Photograph of Cold Flow Experimental Apparatus
3. Schematic of Cold Flow Experimental Setup
4. Photograph of Cold Flow Test Chamber
5. Cold Flow Injector Type
6. Close-Up of Streak Camera
7. Spray Pattern at Various Chamber Pressures
8. Cold Flow Data - Frequency vs. Chamber Pressure
9. Empirical Data Correlation
10. Typical Pressure Trace of Intermediate Frequency
11. Photograph of Combustion Instability Rocket Motor Experimental Apparatus
12. Schematic of Rocket Motor Experimental Setup
13. Rocket Motor Injector
14. Pressure Trace of Step Pulse and Instability
15. Streak Velocity Error
16. Photograph of Window Section
17. Characteristic Exhaust Velocity vs. Chamber Length
18. Velocity vs. Chamber Length
19. Streak Photograph of Pulse
20. General Streak Camera Arrangement
21. Characteristic Exhaust Velocity vs. Chamber Gas Velocity



*Spray Pattern
and Wave Phenomenon*

Figure 1



*Cold Flow
Experimental Setup*

Schematic of Cold Flow Experimental Setup

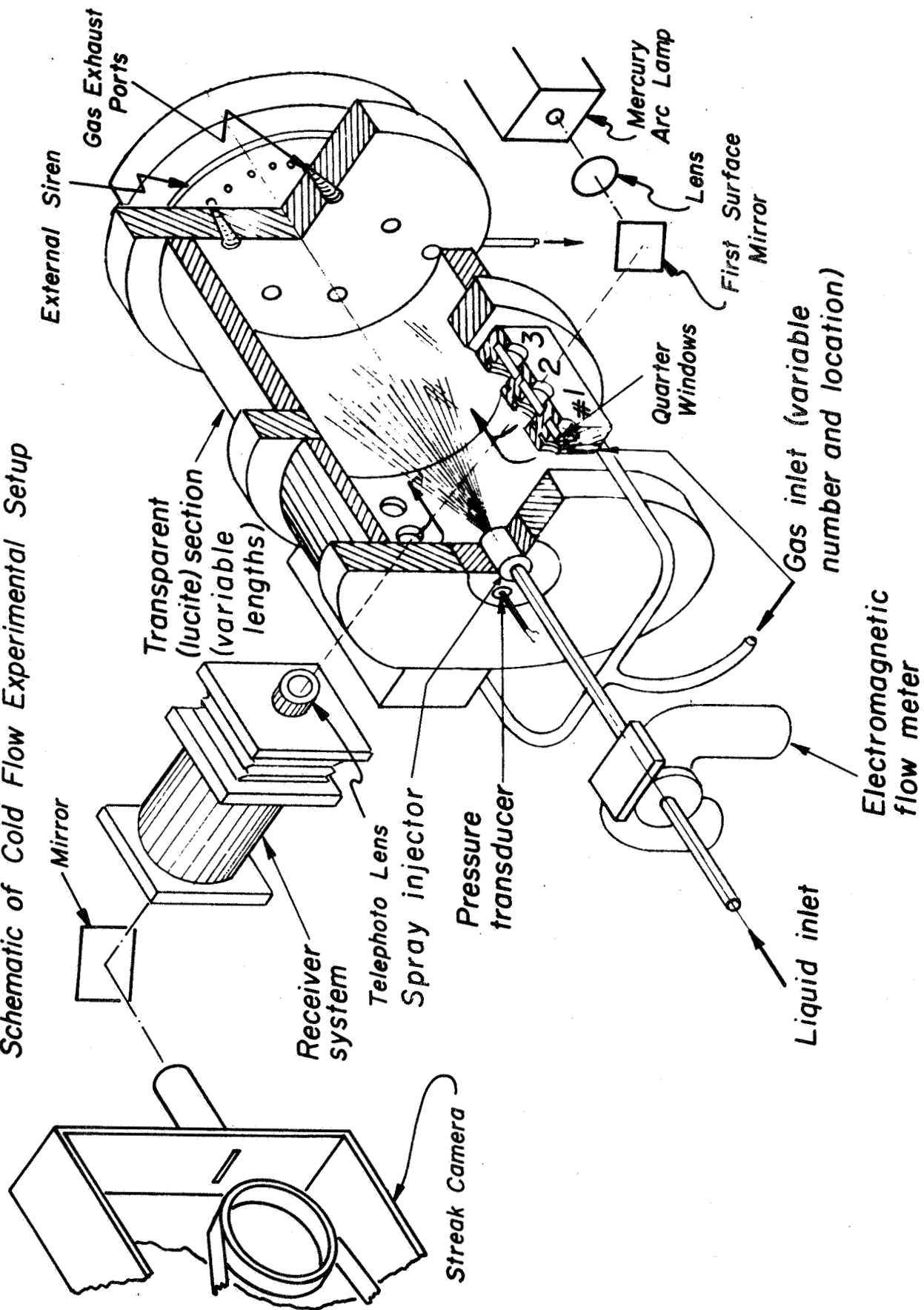
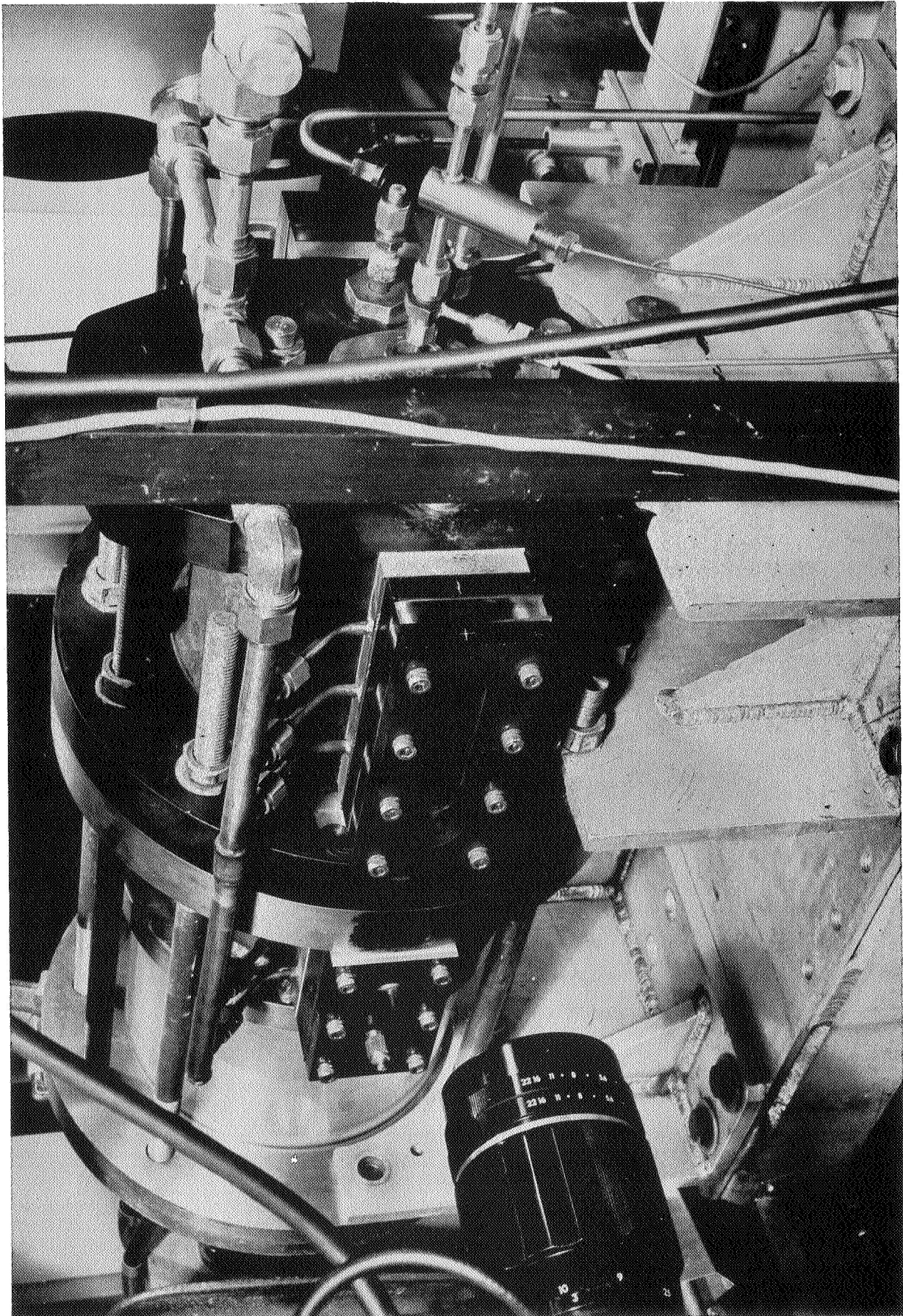


Figure 3



*Cold Flow
Test Chamber*

Figure 4

Impinging jet injector element

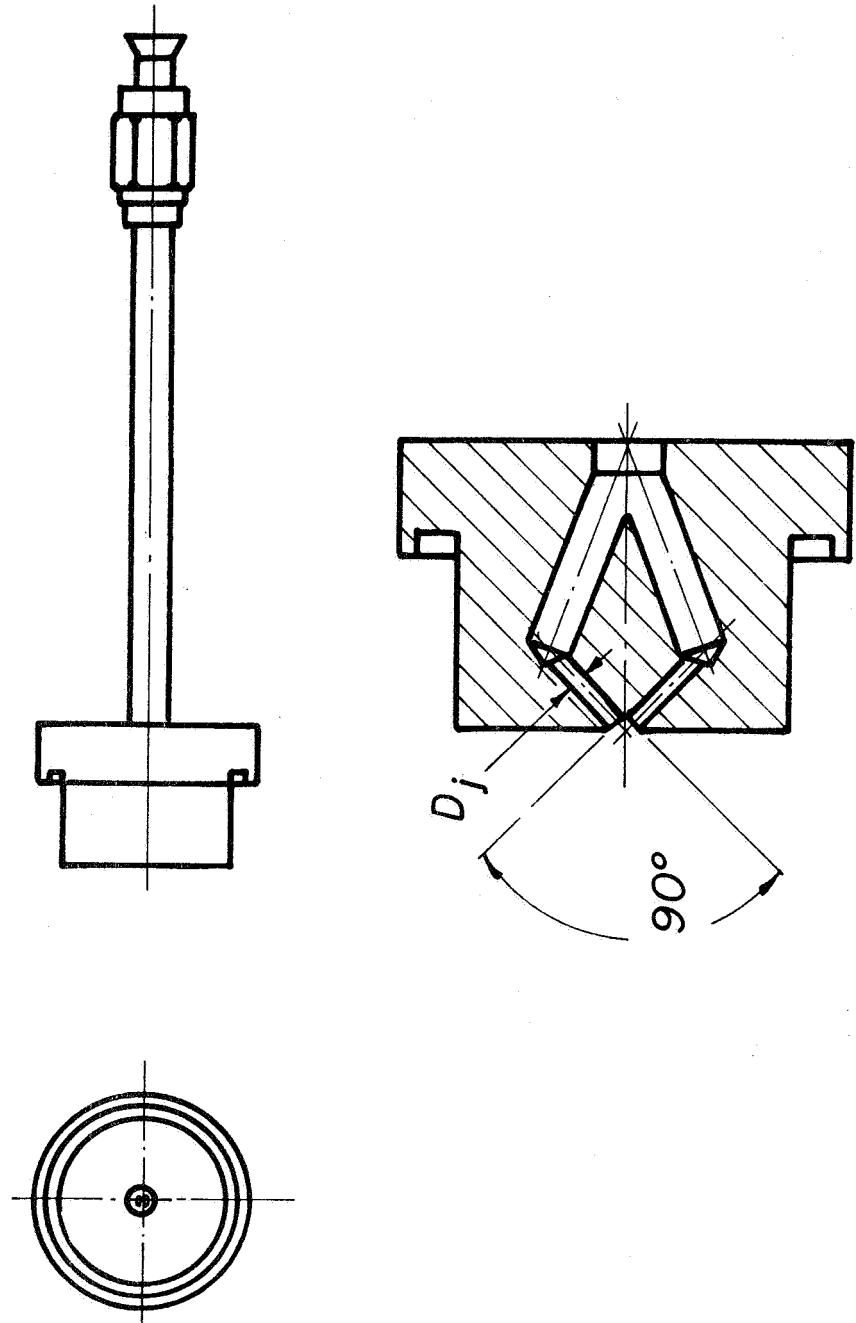
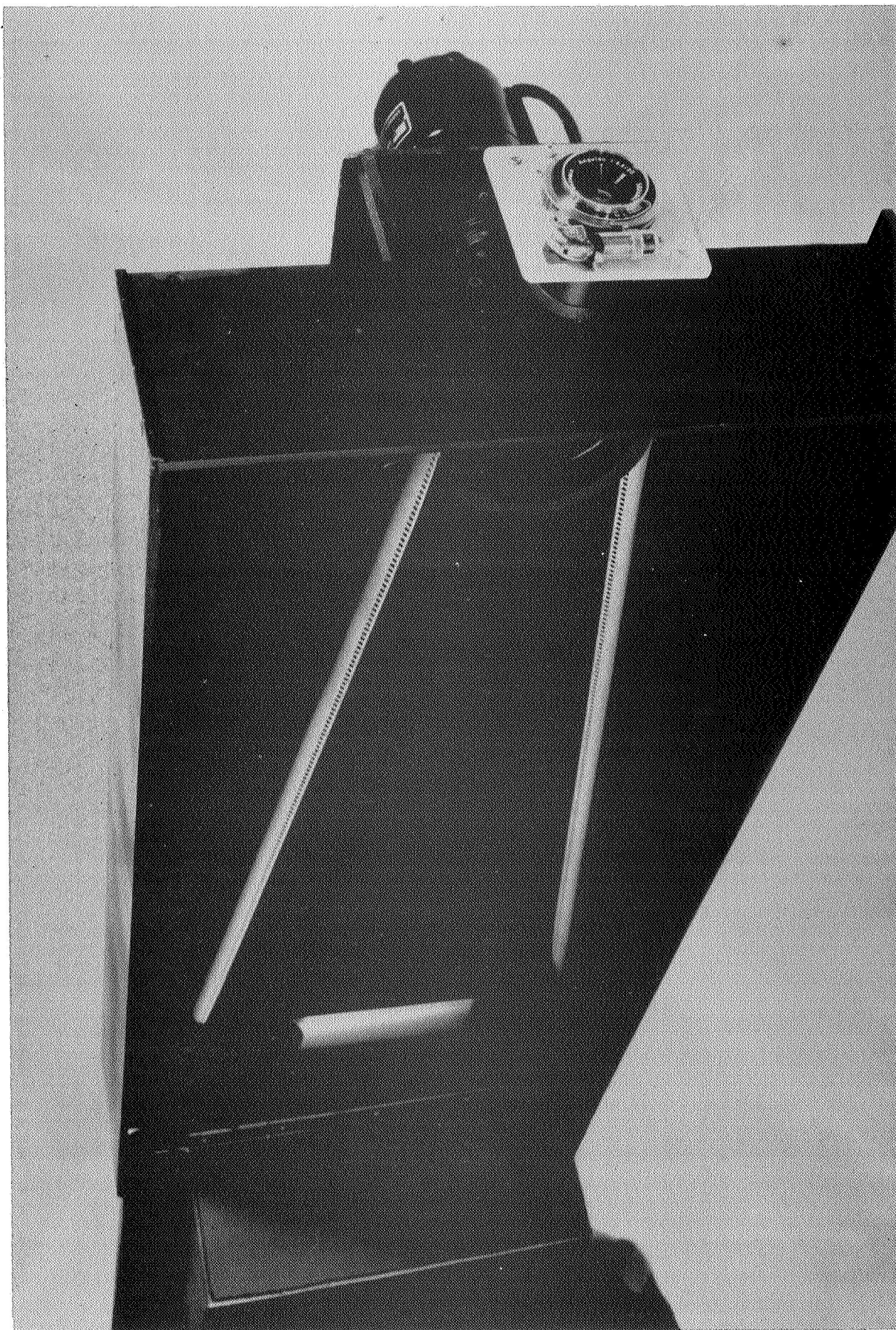


Figure 5

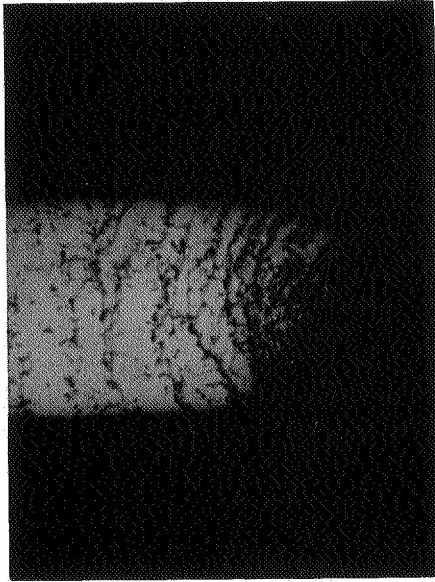
JP21 P61 67



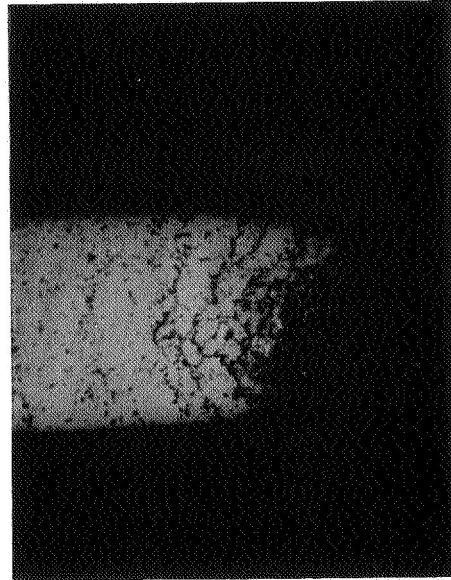
Streak Camera

Figure 6

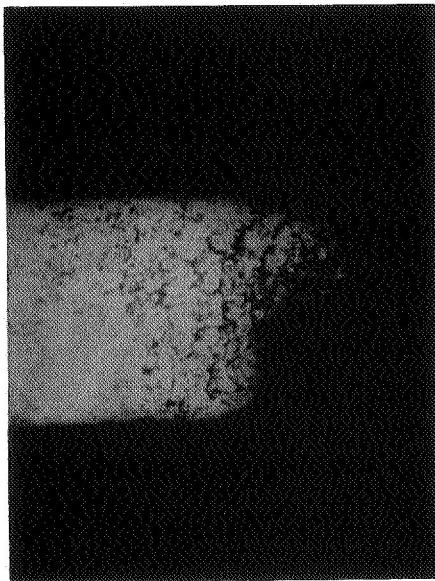
*Impinging injector spray patterns
90°-040" (like-on-like), water, $\Delta P = 50$ psi*



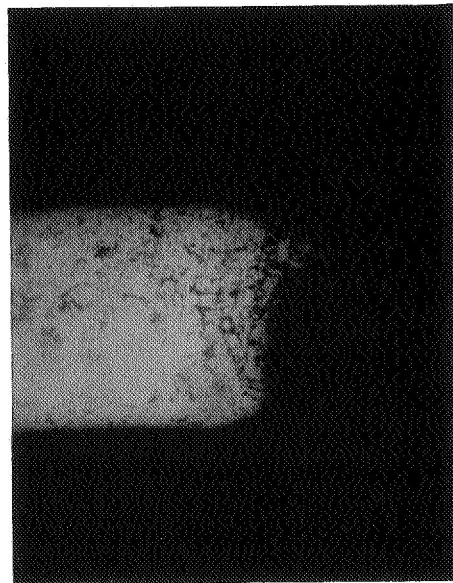
$P_c = 0$ PSIG



$P_c = 20$ PSIG



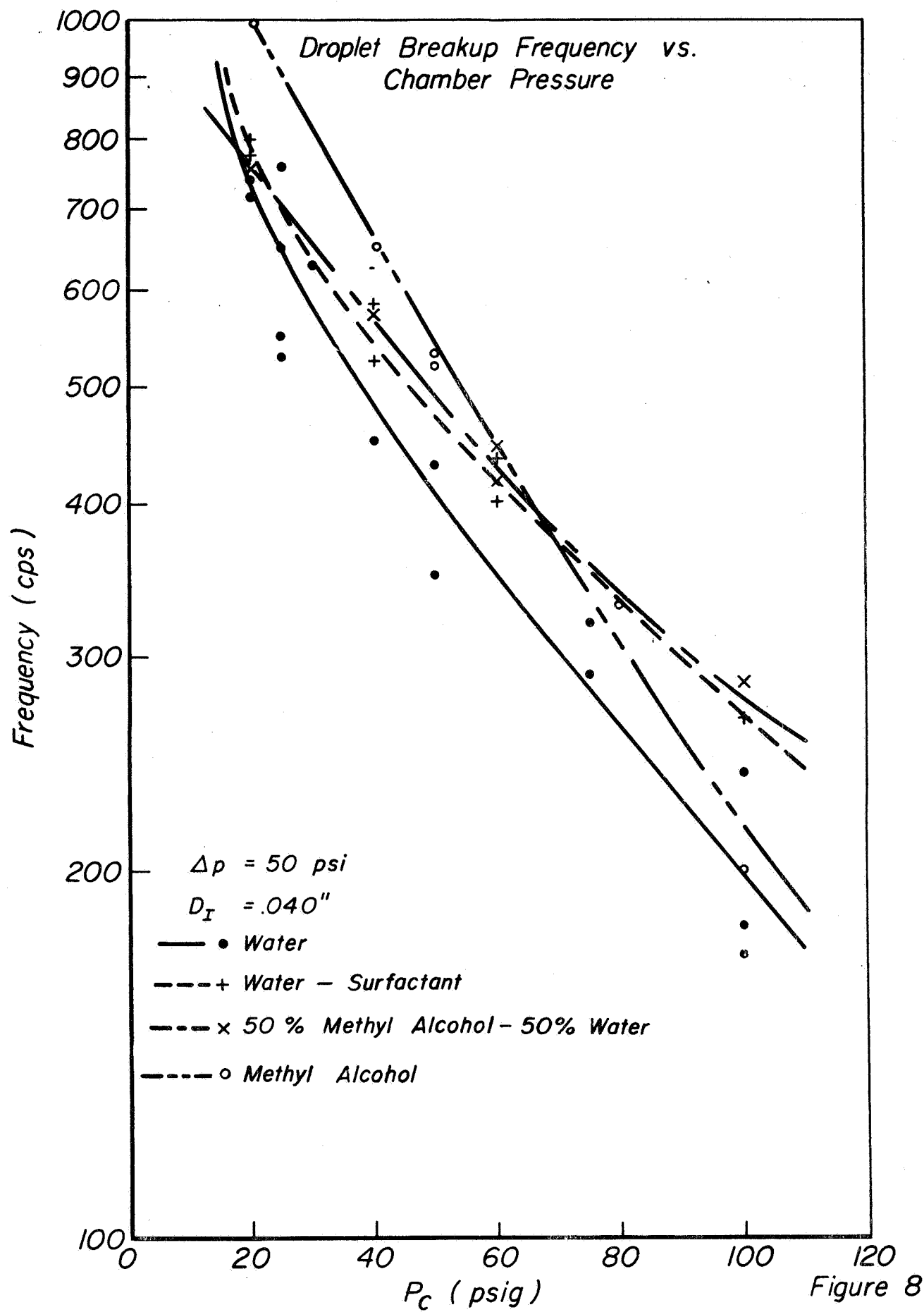
$P_c = 60$ PSIG



$P_c = 80$ PSIG

Figure 7

JP21 E 4261-67



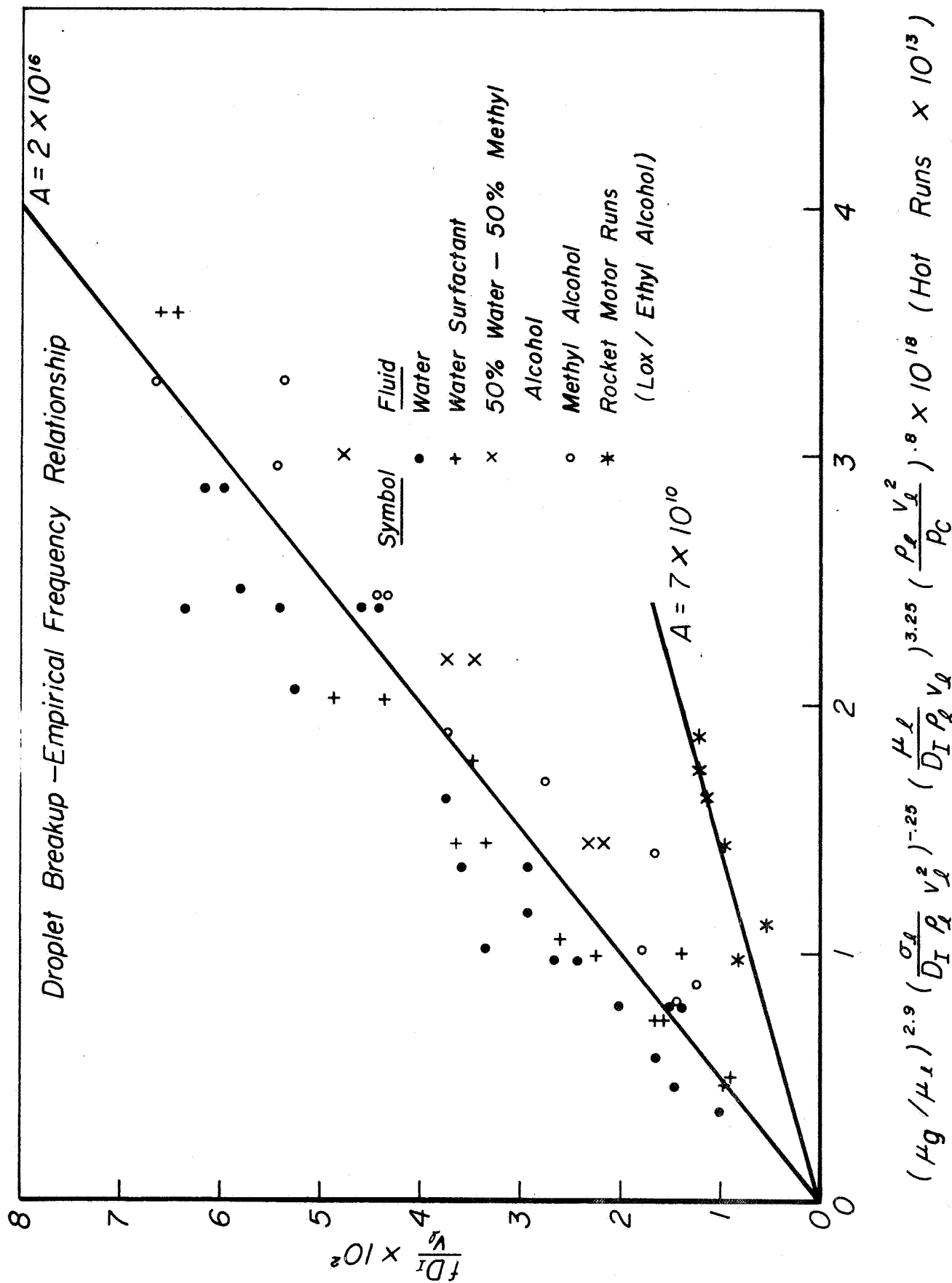


Figure 9

Test firing on transverse stand showing intermediate frequency incidence, $P_c = 134$ psia, $D_c = 9$ ins., $r = 1.95$, 12 spud injector

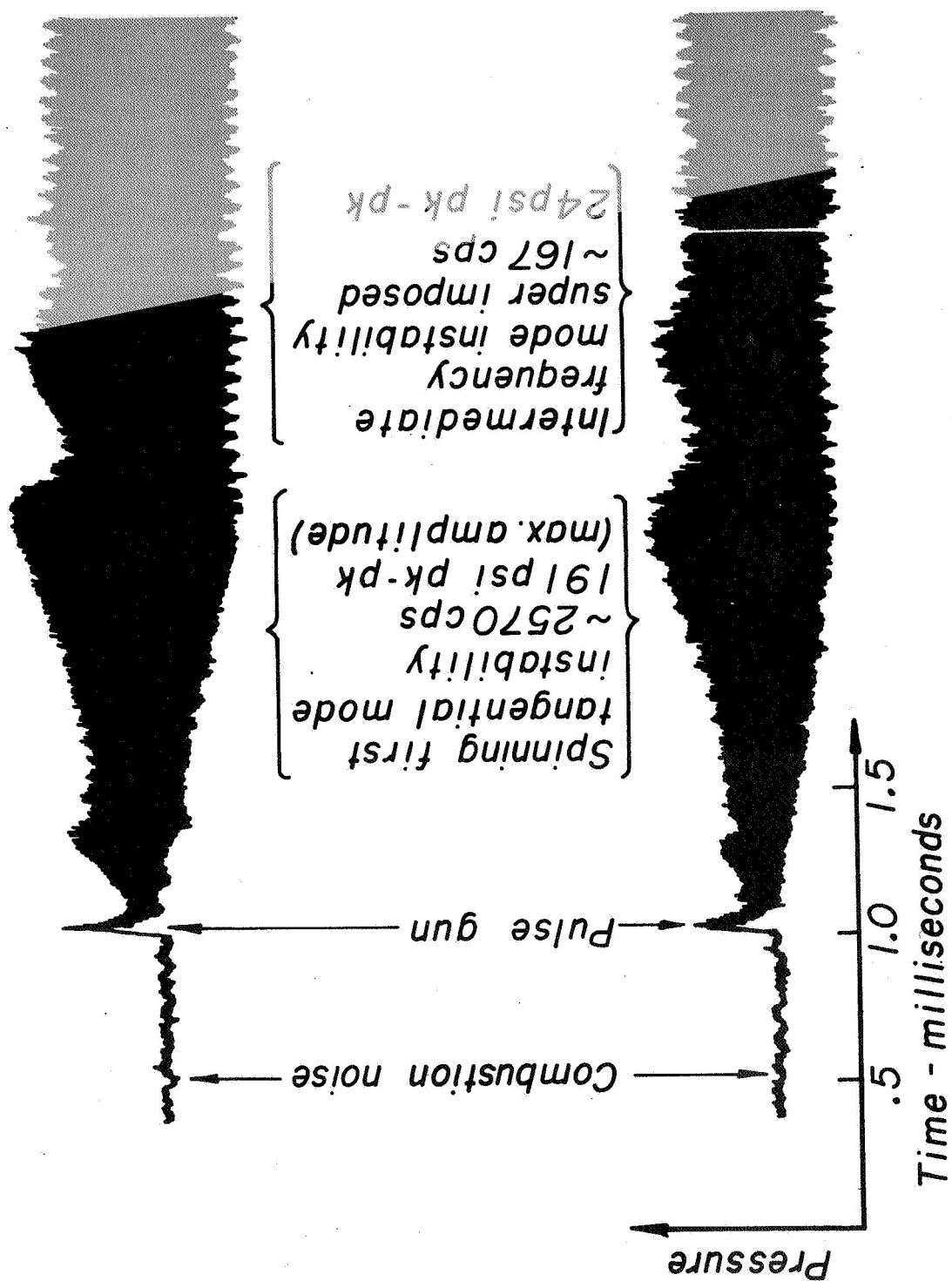
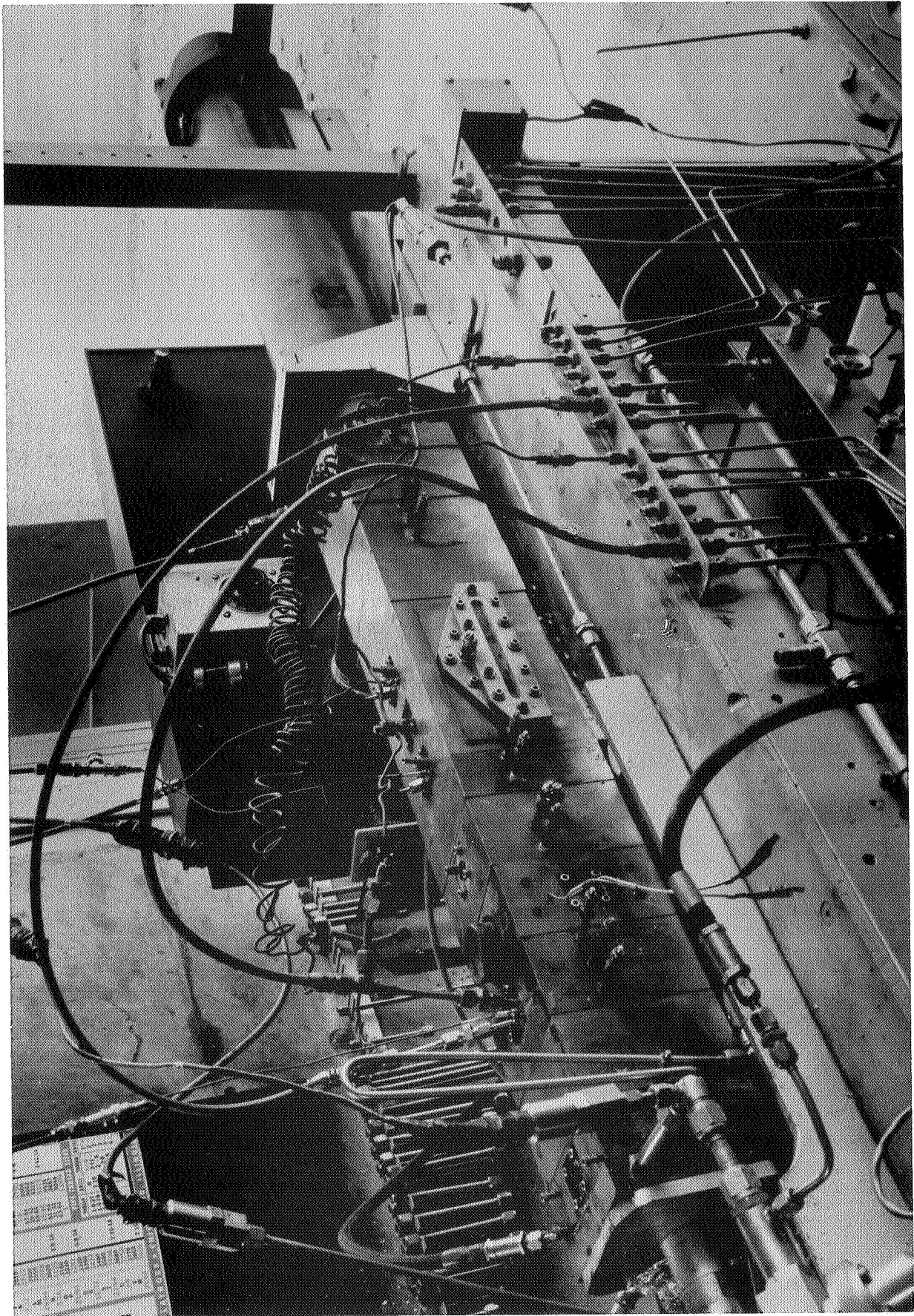


Figure 10



Rocket Motor
Assembly

Figure 11

Schematic of Rocket Motor Experimental Setup

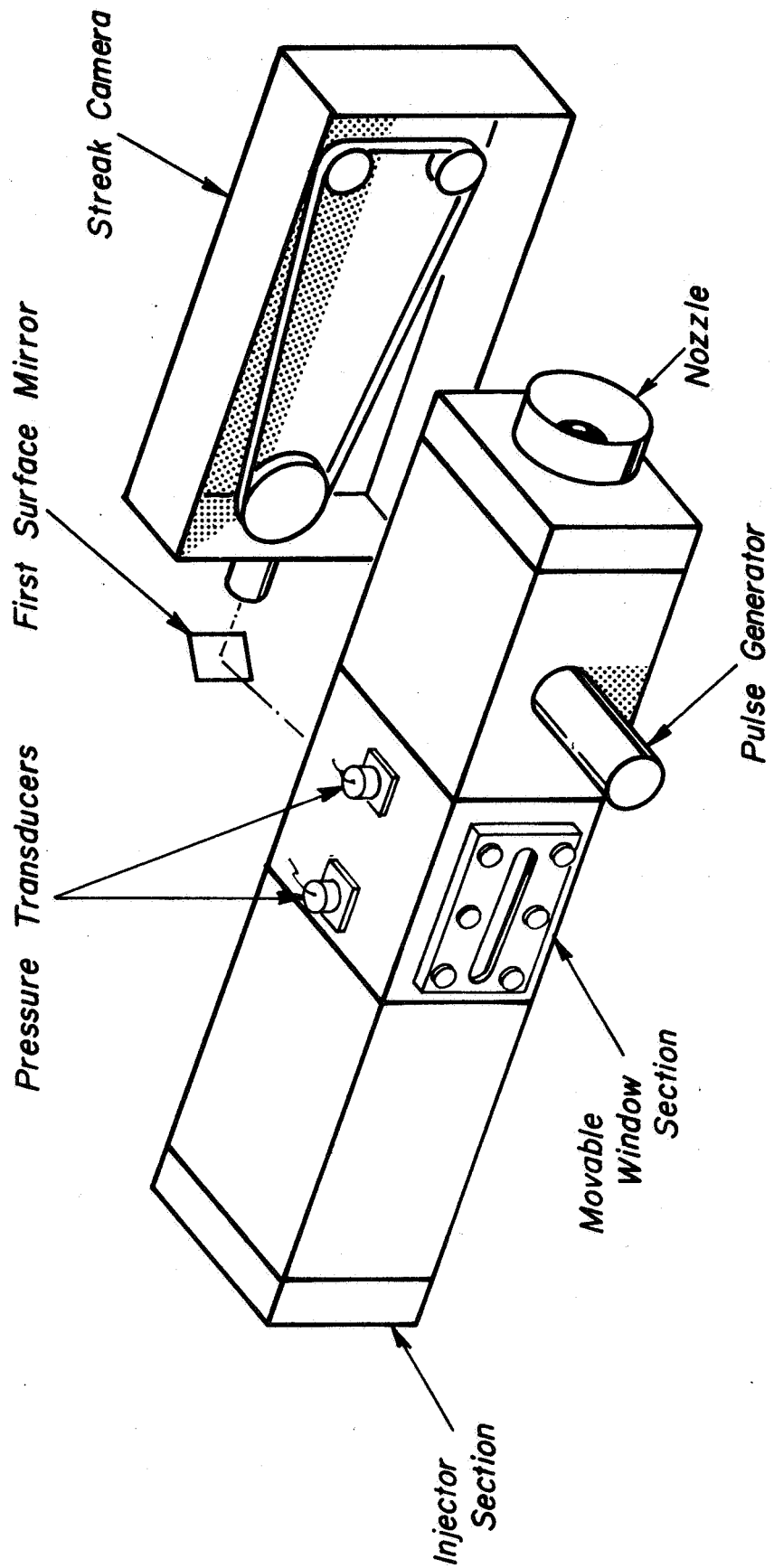
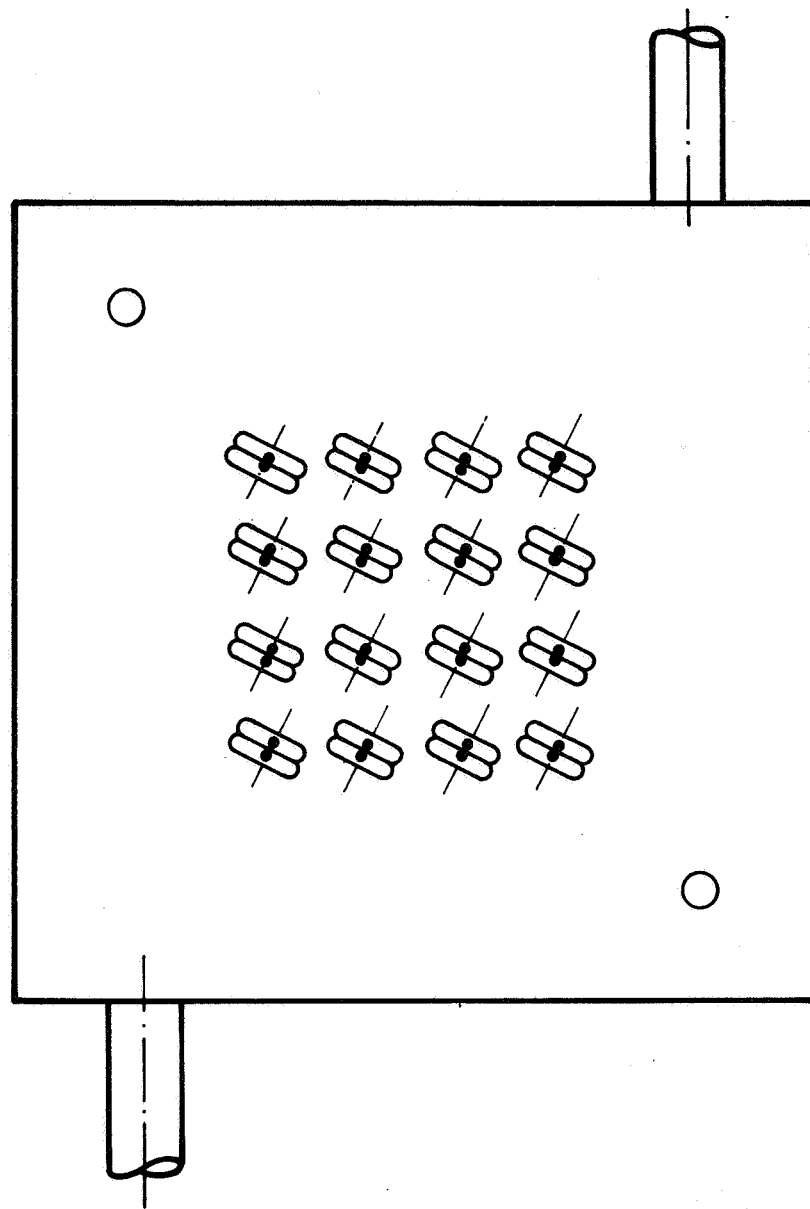


Figure 12



Rocket Motor Injector

Figure 13

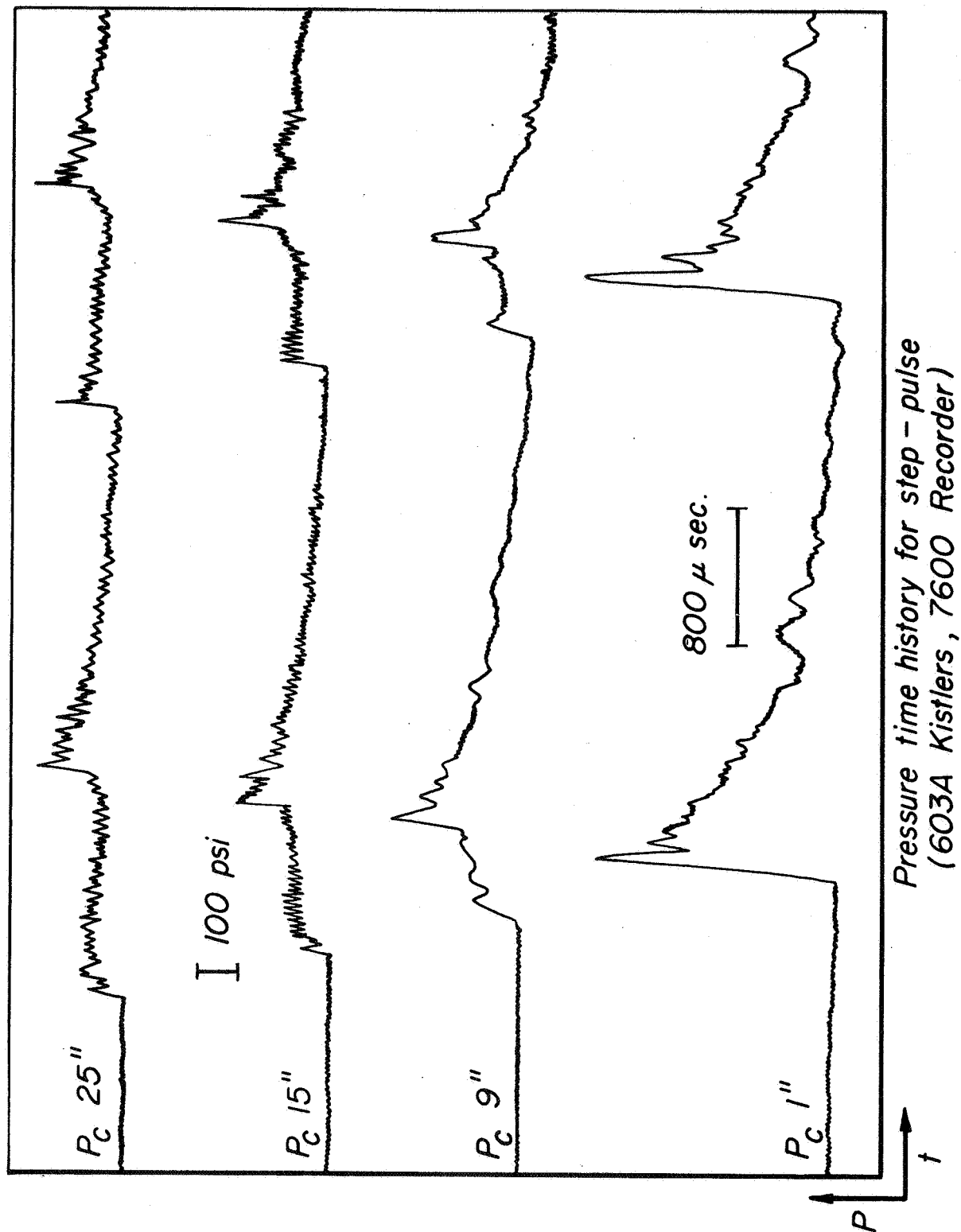
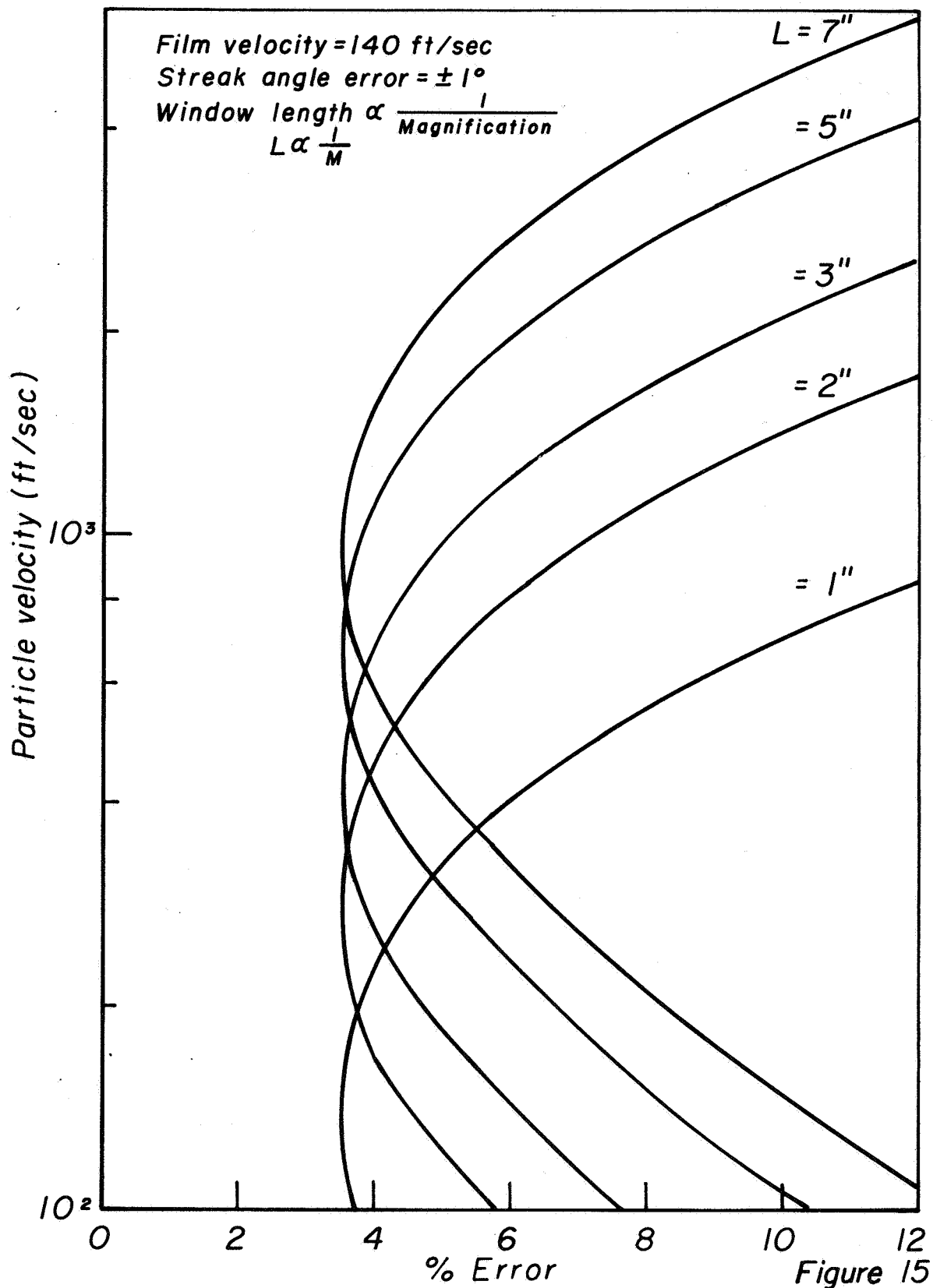
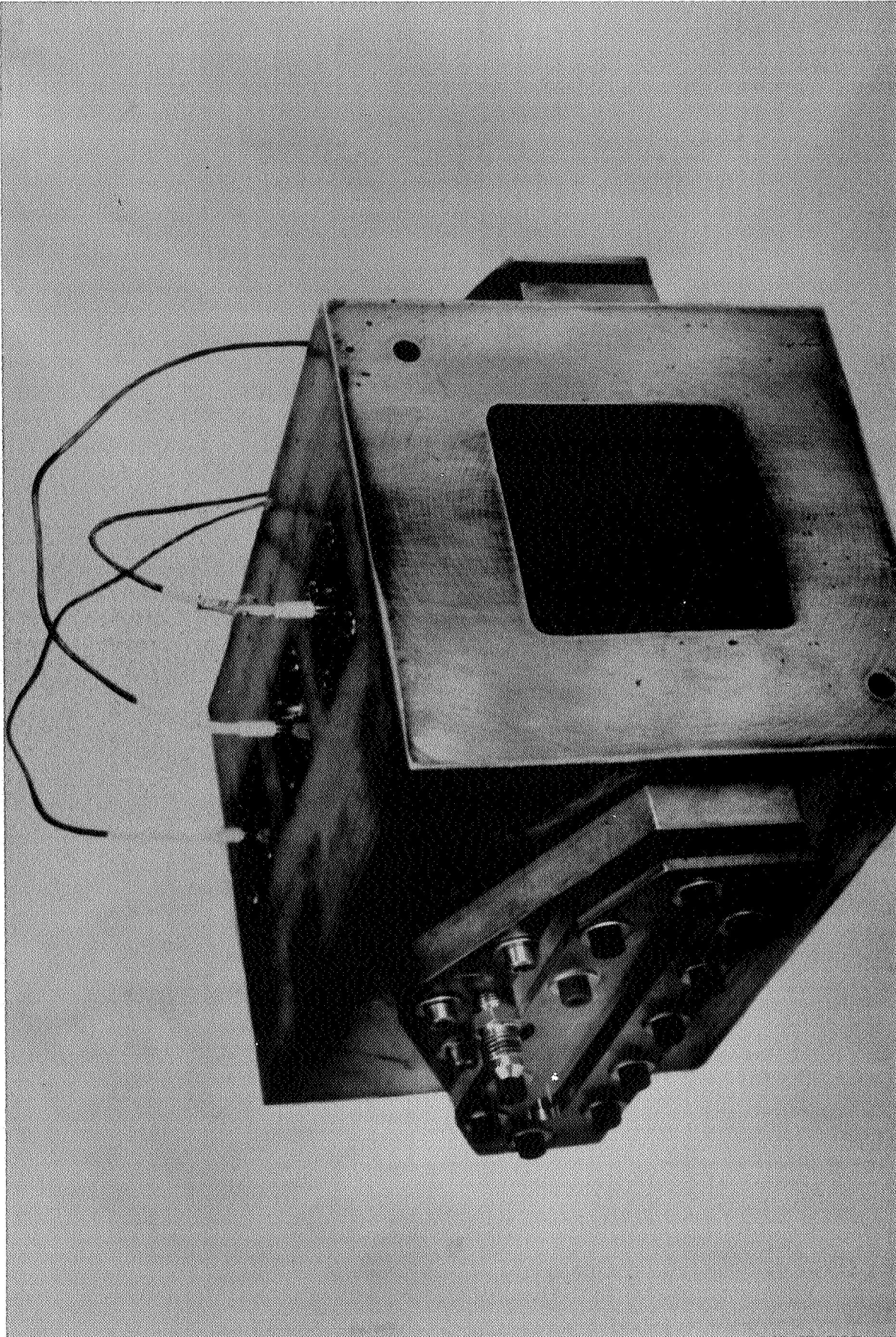


Figure 14

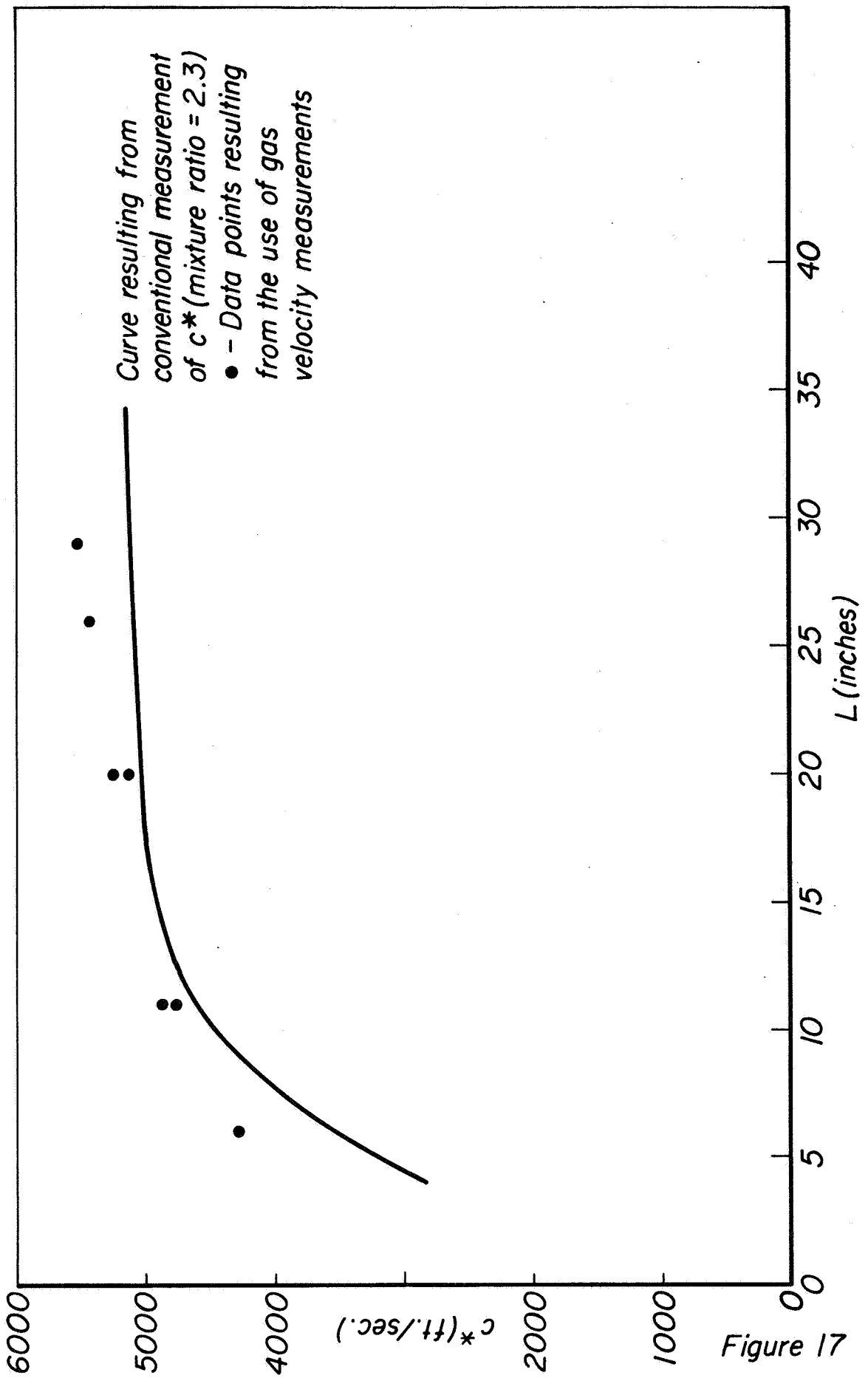
Streak particle velocity vs percentage error





Window Section

Figure 16



Velocity vs Length

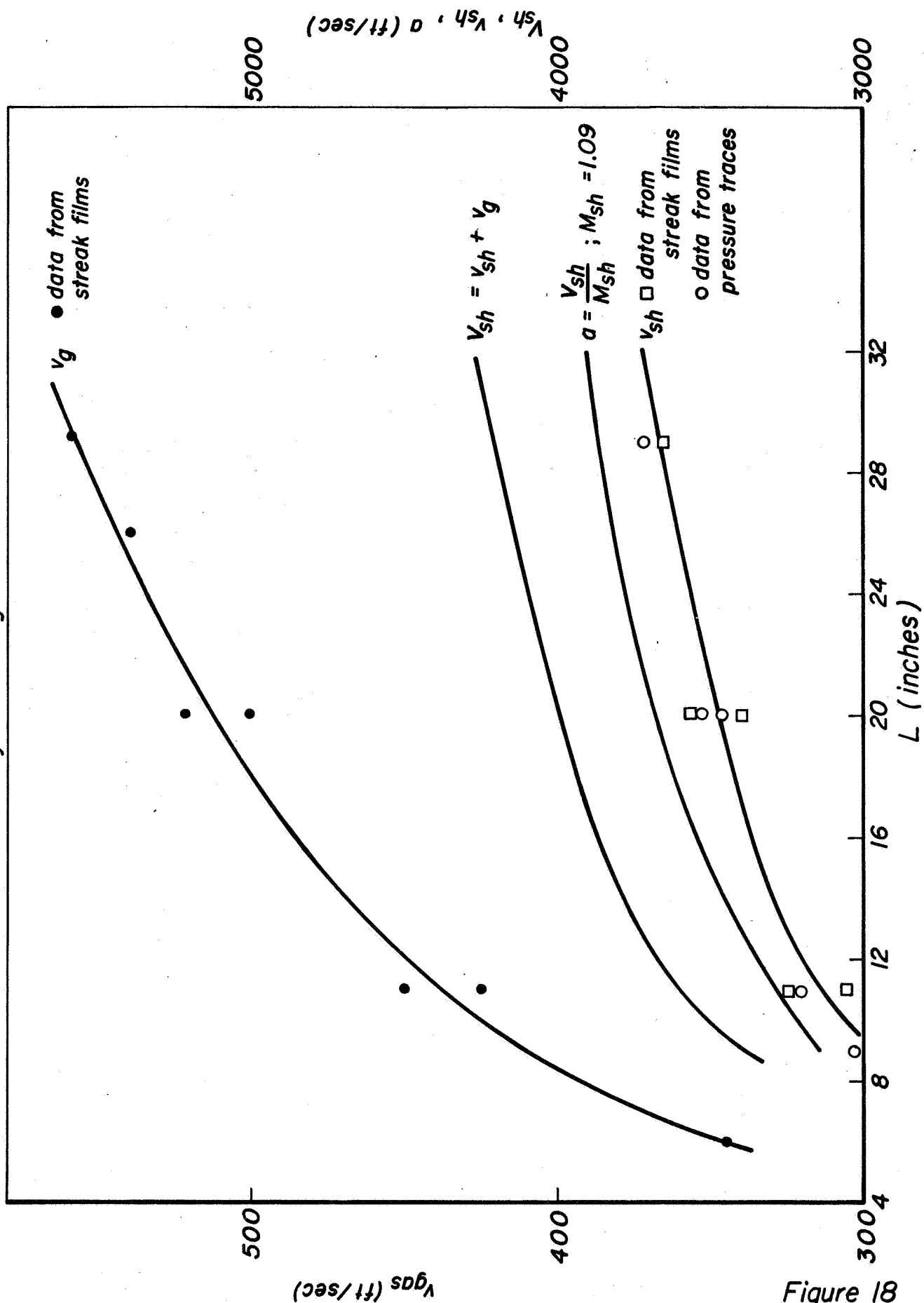
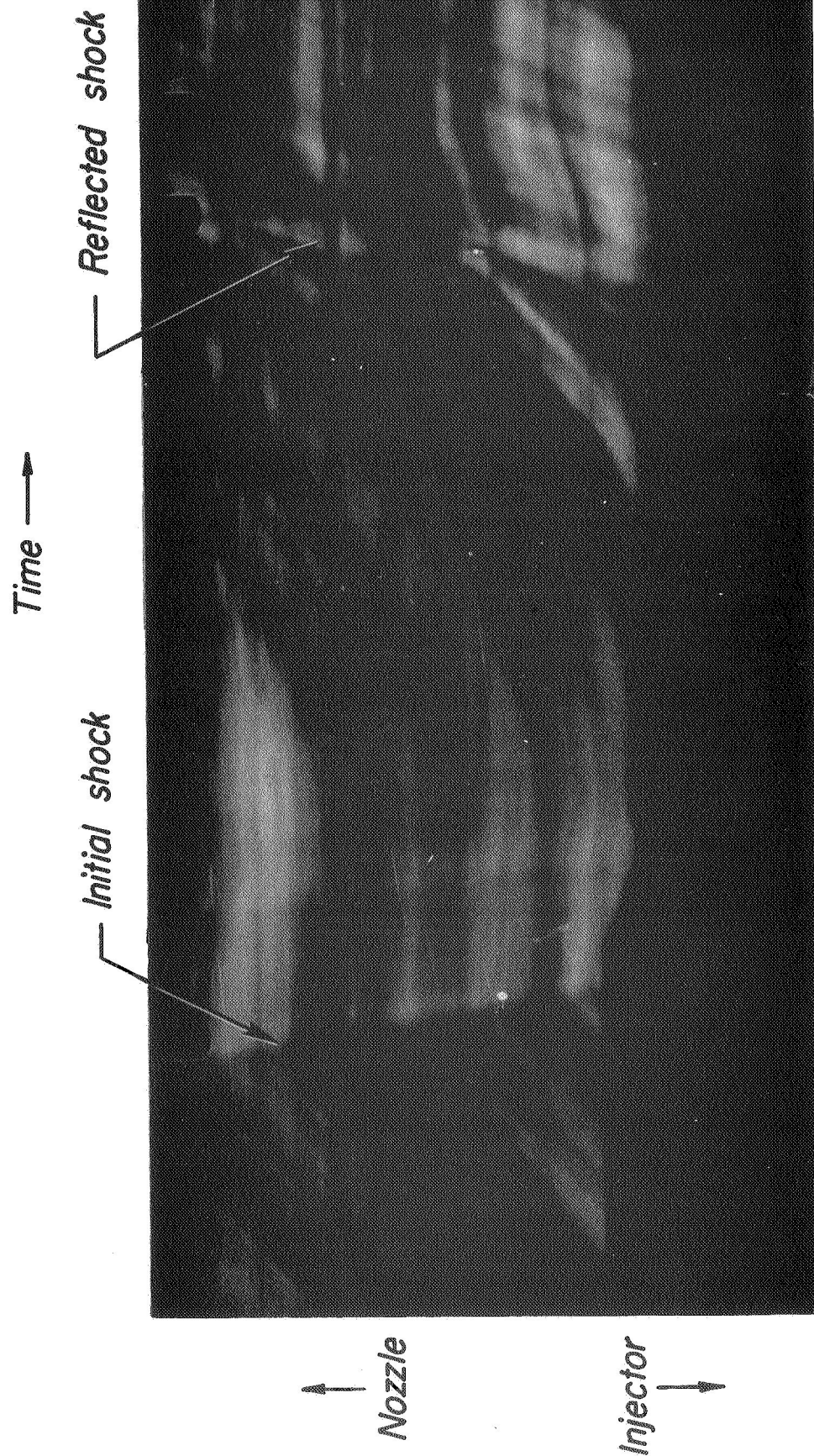


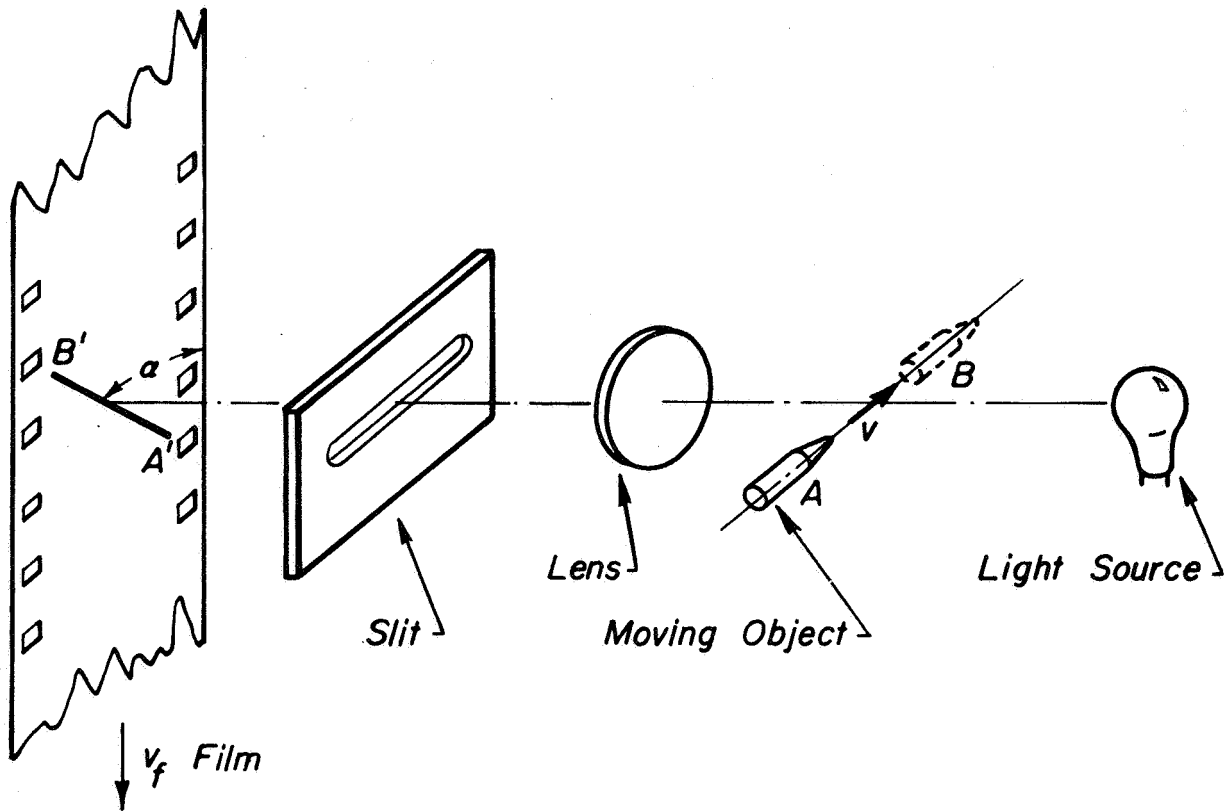
Figure 18



Streak Photograph
of Pulse

Figure 19

General Streak Camera Arrangement



$$M = \frac{A'B' \sin \alpha}{AB}$$

$$v = \frac{v_f \tan \alpha}{M}$$

Figure 20

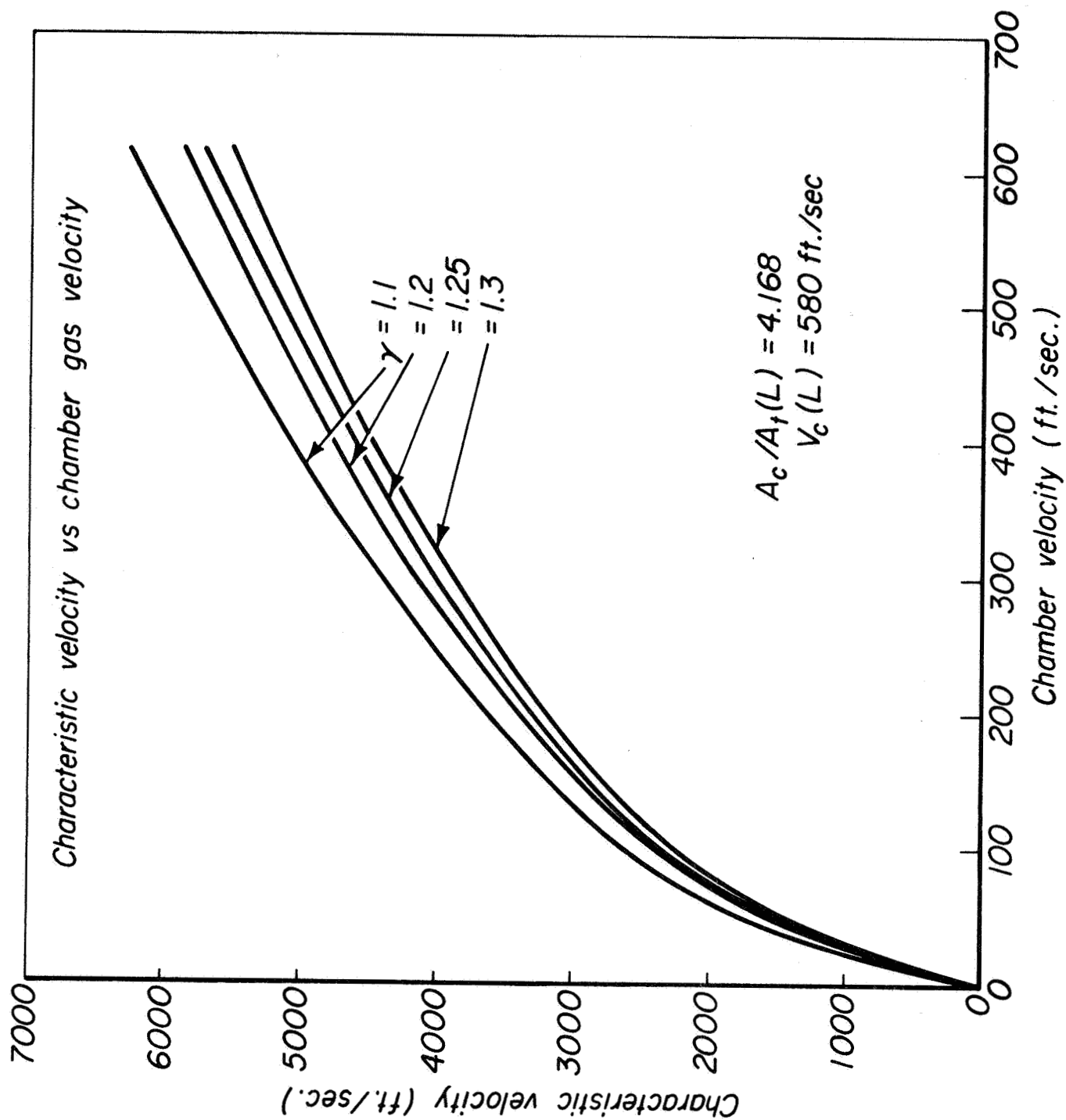


Figure 21

DISTRIBUTION FOR THIS REPORT

NASA

NASA Headquarters
Washington, D.C. 20546
Attn: Mr. A. Gessow
Attn: Dr. R.S. Levine RPL (3)
Attn: Mr. A.O. Tischler RP

NASA
Universal North Building
Connecticut & Florida Avenues
Washington, D.C.
Attn: Dr. T.L. Smull, Director
Grants & Space Contracts (10)

NASA Scientific & Technical
Information Facility
P.O. Box 33
College Park, Maryland 20740 (15)

NASA Headquarters
Washington, D.C. 20546
Attn: Mr. E.L. Gray, Director
Advanced Manned Missions, MT
Office of Manned Space Flight

Attn: Mr. V.L. Johnson, Director
Launch Vehicles & Propulsion, SV
Office of Space Science

Ames Research Center
Moffett Field
California 94035
Attn: Technical Librarian

Goddard Space Flight Center
Greenbelt, Maryland 20771
Attn: Technical Librarian

Jet Propulsion Laboratory
California Institute of Technology
4800 Oak Grove Drive
Pasadena, California 91103
Attn: Mr. J.H. Rupe
Attn: Technical Librarian

John F. Kennedy Space Center, NASA
Cocoa Beach, Florida 32931
Attn: Technical Librarian

Langley Research Center
Langley Station
Hampton, Virginia 23365
Attn: Technical Librarian

NASA
Lewis Research Center
21000 Brookpark Road
Cleveland, Ohio 44135
Attn: Mr. M.F. Heidmann
(Technical Monitor)
Attn: Dr. R.J. Priem
Attn: Mr. E.W. Conrad
Attn: Report Control
Attn: Technical Librarian

Manned Spacecraft Center
Houston, Texas 77001
Attn: Mr. G. Spencer
Attn: Technical Librarian

Marshall Space Flight Center
R-P&VED
Huntsville, Alabama 35812
Attn: Mr. J. Thomson
Attn: Mr. R.J. Richmond
Attn: Technical Librarian

GOVERNMENT INSTALLATIONS

Headquarters, U.S. Air Force
Washington 25, D.C.
Attn: Technical Librarian

Aeronautical Systems Division
Air Force Systems Command
Wright-Patterson Air Force Base
Dayton, Ohio 45433
Attn: Technical Librarian

Air Force Missile Test Center
Patrick Air Force Base
Florida
Attn: Technical Librarian

AFOSR-Propulsion Division
1400 Wilson Boulevard
Arlington, Virginia 22209
Attn: Dr. B.T. Wolfson

Air Force Rocket Propulsion Laboratory
Research & Technology Division
Air Force Systems Command
Edwards, California 93523
Attn: Mr. R.R. Weiss, RPRR
Attn: Mr. B.R. Bornhorst
Attn: Technical Librarian

SAMSO (SMSDI-STINFO)
AF Unit Post Office
Los Angeles, California 90045
Attn: Technical Librarian

ARL (ARC)
Building 450
Wright-Patterson Air Force Base
Dayton, Ohio
Attn: Dr. K. Scheller

Arnold Engineering Development Center
Arnold Air Force Station
Tullahoma, Tennessee
Attn: Technical Librarian

Department of the Navy
Bureau of Naval Weapons
Washington, D.C. 20360
Attn: Technical Librarian

Department of the Navy
Office of Naval Research
Washington, D.C. 20360
Attn: Mr. R.D. Jackel

Defense Documentation Center Headquarters
Cameron Station, Building 5
5010 Duke Street
Alexandria, Virginia 22314
Attn: TISIA

Naval Ordnance Station
Research & Development Dept.
Indian Head, Maryland 20640
Attn: Dr. L.A. Dickinson

Picatinny Arsenal
Dover, New Jersey 07801
Attn: Mr. E. Jenkins
Attn: Technical Librarian

Redstone Scientific Information
Building 4484
Redstone Arsenal
Huntsville, Alabama
Attn: Technical Librarian

RTNT
Bolling Field
Washington, D.C. 20332
Attn: Dr. L. Green, Jr.

U.S. Army Missile Command
Redstone Arsenal
Huntsville
Alabama 35809
Attn: Mr. J. Connaughton
Attn: Technical Librarian

U.S. Atomic Energy Commission
Technical Information Services
Box 62
Oak Ridge, Tennessee
Attn: Technical Librarian

U.S. Naval Ordnance Test Station
China Lake
California 93557
Attn: Mr. T. Inouye
Attn: Technical Librarian

CPIA

Chemical Propulsion Information Agency
Applied Physics Laboratory
The John Hopkins University
8621 Georgia Avenue
Silver Spring, Maryland 20910
Attn: Mr. T.W. Christian
Attn: Technical Librarian

INDUSTRY CONTRACTORS

Aerojet-General Corporation
P.O. Box 296
Azusa, California 91702
Attn: Dr. R.J. Hefner
Attn: Technical Librarian

Aerojet-General Corporation
P.O. Box 1947
Sacramento, California 95809
Attn: Mr. J.M. McBride
Attn: Technical Librarian
Bldg. 2015, Dept. 2410

Aeronutronic
Philco Corporation
Ford Road
Newport Beach, California 92663
Attn: Technical Librarian

Aerospace Corporation
P.O. Box 95085
Los Angeles, California 90045
Attn: Mr. O.W. Dykema
Attn: Technical Librarian

Astrosystems International, Inc.
1275 Bloomfield Avenue
Fairfield, New Jersey 07007
Attn: Technical Librarian

Atlantic Research Corporation
Edsall Road and Shirley Highway
Alexandria, Virginia 22314
Attn: Technical Librarian

Autonetics
Div. of North American Aviation, Inc.
3370 Miraloma Avenue
Anaheim, California 92803
Attn: Dr. J.C. Chu

Battelle Memorial Institute
505 King Avenue
Columbus 1, Ohio 43201
Attn: Mr. C.E. Day,
Classified Rept. Librarian

Bell Aerosystems Company
P.O. Box 1
Buffalo 5, New York 14240
Attn: Dr. K. Berman
Attn: Mr. J.M. Senneff
Attn: Technical Librarian

Boeing Company
P.O. Box 3707
Seattle, Washington 98124
Attn: Technical Librarian

Bolt, Berenak & Newman, Inc.
Cambridge, Massachusetts
Attn: Dr. I. Dyer

Chrysler Corporation
Missile Division
P.O. Box 2628
Detroit, Michigan 48231
Attn: Technical Librarian

Curtiss-Wright Corporation
Wright Aeronautical Division
Wood-Ridge, New Jersey 07075
Attn: Technical Librarian

Defense Research Corporation
6300 Hollister Avenue
P.O. Box 3587
Santa Barbara, California 93105
Attn: Dr. C.H. Yang

Douglas Aircraft Company
Missile & Space Systems Division
3000 Ocean Park Boulevard
Santa Monica, California 90406
Attn: Technical Librarian

Douglas Aircraft Company
Astropower Laboratory
2121 Paularino
Newport Beach, California 92663
Attn: Technical Librarian

Dynamic Science Corporation
1900 Walker Avenue
Monrovia, California 91016
Attn: Mr. R.J. Hoffman

General Dynamics/Astronautics
Library & Information Services (128-00)
P.O. Box 1128
San Diego, California 92112
Attn: Technical Librarian

General Electric Company
Advanced Engine & Technology Dept.
Cincinnati, Ohio 45215
Attn: Technical Librarian

General Electric Company
Malta Test Station
Ballston Spa, New York 12020
Attn: Dr. A. Graham, Manager
Rocket Engines

General Electric Company
Re-Entry Systems Department
3198 Chestnut Street
Philadelphia, Pennsylvania 19101
Attn: Technical Librarian

Geophysics Corporation of America
Technical Division
Bedford, Massachusetts 01734
Attn: Mr. A.C. Toby

Grumman Aircraft Engineering Corp.
Bethpage
Long Island, New York 11714
Attn: Technical Librarian

Institute for Defense Analyses
RESA
400 Army-Navy Drive
Arlington, Virginia 22202
Attn: Dr. W.C. Strahle

Ling-Temco-Vought Corporation
Astronautics
P.O. Box 5907
Dallas, Texas 75222
Attn: Technical Librarian

Arthur D. Little, Inc.
20 Acorn Park
Cambridge, Massachusetts 02140
Attn: Technical Librarian

Lockheed Missiles & Space Co.
P.O. Box 504
Sunnyvale, California 94088
Attn: Technical Information Center

Lockheed Propulsion Company
P.O. Box 111
Redlands, California 91409
Attn: Technical Librarian

McDonnell Aircraft Corporation
P.O. Box 516
Municipal Airport
St. Louis, Missouri 63166
Attn: Technical Librarian

The Marquardt Corporation
16555 Saticoy Street
Van Nuys, California 91409
Attn: Technical Librarian

Martin Marietta Corporation
Denver Division
P.O. Box 179
Denver, Colorado 80201
Attn: Technical Librarian

Multi-Tech. Inc.
Box 4186 No. Annex
San Fernando, California
Attn: Mr. F.B. Cramer

Northrup Space Laboratories
3401 West Broadway
Hawthorne, California 90250
Attn: Technical Librarian

Rocket Research Corporation
520 South Portland Street
Seattle, Washington 98108
Attn: Technical Librarian

Rocketdyne
Division of North American Aviation
6633 Canoga Avenue
Canoga Park, California 91304
Attn: Mr. R. Fontaine
Attn: Dr. R.B. Lawhead
Attn: Technical Librarian
(Library 586-306)

Space & Information Systems Division
North American Aviation, Inc.
12214 Lakewood Boulevard
Downey, California 90241
Attn: Technical Librarian

Rohm & Haas Company
Redstone Arsenal
Huntsville, Alabama
Attn: Librarian

Stanford Research Institute
333 Ravenswood Avenue
Menlo Park, California 94025
Attn: Dr. G. Marxman

Thiokol Chemical Corporation
Huntsville Division
Huntsville, Alabama
Attn: Technical Librarian

Thiokol Chemical Corporation
Reaction Motors Division
Denville, New Jersey 07834
Attn: Mr. D. Mann
Attn: Technical Librarian

TRW Systems
One Space Park
Redondo Beach, California 90278
Attn: Mr. G.W. Elverum
Attn: Mr. D.H. Lee
Attn: Technical Librarian

United Technology Center
Division of United Aircraft Corporation
P.O. Box 358
Sunnyvale, California 94088
Attn: Mr. R.H. Osborn
Attn: Technical Librarian

Pratt & Whitney Aircraft Company
Division of United Aircraft Corp.
West Palm Beach
Florida
Attn: Mr. G. Lewis

Pratt & Whitney Aircraft Company
Division of United Aircraft Corp.
Engineering, Building 1-F
East Hartford, Connecticut
Attn: Mr. D.H. Utvik

Research Laboratories
Division of United Aircraft Corp.
400 Main Street
East Hartford, Connecticut 06108
Attn: Technical Librarian

Walter Kidde and Company
Aerospace Operations
567 Main Street
Belleville, New Jersey 07109
Attn: Technical Librarian

Warner-Swasey Company
Control Instrument Division
32-16 Downing Street
Flushing, New York 11354
Attn: Dr. R.H. Tourin

UNIVERSITIES

California Institute of Technology
204 Karman Laboratory
Pasadena, California 91109
Attn: Prof. F.E. Culick

Case Institute of Technology
Engineering Division
University Circle
Cleveland, Ohio 44106
Attn: Prof. C.R. Klotz

Dartmouth University
Hanover
New Hampshire 03755
Attn: Prof. P.D. McCormack

Georgia Institute of Technology
Aerospace School
Atlanta 13
Georgia 30332
Attn: Prof. B.T. Zinn
Prof. E.W. Price

Illinois Institute of Technology
10 W. 35th Street
Chicago, Illinois 60616
Attn: Dr. P.T. Torda

The Johns Hopkins University
Applied Physics Laboratory
8621 Georgia Avenue
Silver Spring, Maryland 20910
Attn: Dr. W.G. Berl

Massachusetts Institute of Technology
Cambridge 39
Massachusetts 02139
Attn: Prof. T.Y. Toong
Dept. of Mechanical Engineering
Attn: Gail E. Partridge, Librarian
Engineering Projects Laboratory

New York University
Dept. of Chemical Engineering
New York 53, New York
Attn: Prof. P.F. Winternitz

Ohio State University
Rocket Research Laboratory
Dept. of Aeronautical
and Astronautical Eng.
Columbus 10, Ohio 42310
Attn: Technical Librarian

Polytechnic Institute of Brooklyn
Graduate Center
Route 110
Farmingdale, New York 11735
Attn: Prof. V.D. Agosta

Purdue University
School of Mechanical Engineering
Lafayette, Indiana 47907
Attn: Prof. J.R. Osborn

Sacramento State College
Engineering Division
60000 J. Street
Sacramento, California 95819
Attn: Prof. F.H. Reardon

Sheffield University
Research Laboratories
Harpur Hill
Buxton, Derbyshire
England
Attn: Dr. V.J. Ibberson

University of California
Department of Chemical Engineering
6161 Etcheverry Hall
Berkeley, California 94720
Attn: Prof. A.K. Oppenheim

University of Michigan
Aeronautical & Astronautical Eng. Labs.
Aircraft Propulsion Lab.
North Campus
Ann Arbor, Michigan 48104
Attn: Dr. J.A. Nicholls

University of Southern California
Dept. of Mechanical Engineering
University Park
Los Angeles, California 90007
Attn: Prof. M. Gerstein

University of Wisconsin
Dept. of Mechanical Engineering
1513 University Avenue
Madison, Wisconsin 53705
Attn: Prof. P.S. Myers

Yale University
Dept. of Engineering & Applied Science
Mason Laboratory
400 Temple Street
New Haven, Connecticut
Attn: Prof. B.T. Chu